Experimental Study of Laminated Glass Window Responses under Impulsive and Blast Loading

Xihong Zhang[1]*, Hong Hao[2], and Zhongqi Wang[3]

1. School of Civil, Environmental and Mining Engineering, the University of Western Australia, 35 Stirling Highway, Crawley WA 6009, Australia

2. Tianjin University and Curtin University Joint Research Center for Structure Monitoring and Protection, School of Civil and Mechanical Engineering, Curtin University, Kent Street, Bentley WA 6102, Australia

3. The State Key Laboratory of Explosion Science and Technology, Beijing Institute of Technology, China

*email: xihong.zhang@uwa.edu.au

Abstract

Laminated glass panes are widely adopted as blast-resistant glass windows to mitigate the hazard from ejecting fractured glass fragments. The response of laminated glass windows under blast loads is often predicted by equivalent static analysis or simplified equivalent single degree of freedom (SDOF) analysis. The equivalent SDOF and equivalent static analyses are also respectively adopted in UFC and ASTM design guide for glass window designs. Owing to the inherent problems, the SDOF analysis can only predict the global responses of glass windows and the predictions are not necessarily always satisfactory. Therefore the accuracy and applicability of the SDOF analysis is sometimes questioned. Often numerical simulations and/or experimental tests have to be carried out for reliable predictions of laminated glass window responses to blast loads. In this study, experimental tests on laminated glass windows subjected to impact and blast loads were carried out to evaluate the accuracy of available analyses and design methods. Pendulum impact tests were conducted first on laminated panes of various thicknesses. Full-scale field blast tests were performed on laminated

glass windows of dimension 1.5m × 1.2m. Glass pane deflections were monitored by mechanical linear voltage displacement transducer (LVDT) and high-speed cameras. The responses of the tested windows are compared with the estimations of SDOF models and design standards in this paper. Available blast testing data by other researchers are also included together with the current testing data to evaluate the accuracy of the SDOF and equivalent static analyses defined in the design guides. The adequacy of these simplified approaches in predicting laminated glass window responses to blast loads is discussed.

Keyword: Laminated glass, field blast test, pendulum impact, SDOF

1. Introduction

Glass is ubiquitously used as structural façade and building windows. However, glass is a brittle and fragile material that traditional monolithic glass panes offer little resistance particularly to extreme loads such as impact and air blast loads. Because the fractured glass shards due to blast loads are jagged and flying at high velocities, the failure of glass windows often leads to enormous casualties. The investigation on blast resistant glazing dates back to World War II. A number of retrofit solutions have been introduced [1]. Of the various mitigation measures, laminated glass has been proved to be one of the most direct and effective methods to reduce the risk of glass fragment injuries on the residents. Laminated glazing is made up of two or more layers of glass panes laminated together with one or multiple plies of polymer interlayers. The aim of laminated glass is to prevent shattered glass shards from ejecting towards the residents. After glass cracking, the splinters will be held by the interlayer which with substantial

ductility, deforms significantly as a continuous membrane. The study on laminated glass response to air blast load has been being carried out since it was firstly introduced from automobile to structural glass windows. The Irish terrorism attacks on British barracks during the 1980s and 1990s fueled the substantial investigations and development of laminated glass windows. Empirical design procedures were consequentially drafted based on field blast testing results, which basically defined the minimum required stand-off distance to prevent failure. With more testing data on laminated panes, it was realized that simply interpolating empirical data to windows of other dimensions and different blast loading scenarios other than those tested could lead to enormous errors as non-linear relationship were found between glass window response and the explosion threat. More and thorough studies are therefore deemed necessary to better understand the response of laminated glass and to give more accurate estimation of laminated glass blast loading resistant capacities.

Larcher et al. [2] describes the failure process of laminated glass under lateral pressure in five phases: 1) Glass plies deform elastically; 2) the outer glass ply cracks; 3) the inner glass ply breaks; 4) the PVB interlayer deforms elastically and then plastically; 5) the interlayer fails at ultimate stress (strain) or cut by the glass shards. The above steps outline the general behavior of laminated glass under blast loading. The behavior of pre-cracked laminated glass has been extensively studied by some researchers [3-5]. A major concern is the amount of shear force transferred through the polymer interlayer in the composite laminated pane. Earlier studies were to draw an upper bound to equivalent the total thickness of

laminated pane to a monolithic pane of the same thickness and a lower bound of two glass plies only by assuming no shear transfer through the interlayer. Wei et al. [3] constructed a finite element model of laminated pane using a viscoelastic material model for PVB to investigate the role of interlayer. It was concluded that there were only minor differences in pane deflection and principal stress between laminated glass and monolithic glass of the same thickness. By using a Generalized Maxwell Series model, Duser et al. [4] took the strain-rate effect into consideration in their analysis. It was found that the tensile stress on the outer glass ply was slightly higher than that of an equivalent monolithic pane which marginally increases the possibility of failure initiating on the inner glass pane. Morison [5] summarized relevant previous studies and commented that regardless of the influence of interlayer on stress distribution, which hardly alters the failure probability of laminated pane, for glass pane under large deflection where membrane stress is substantial, the upper and lower bound of laminated pane stiffness breaks down and the probability of failure converges.

The post-crack behavior of laminated glass has been widely studied. Major design guides such as UFC 3-340-02 [6] and Glazing Hazard Guide [7] by Security Facilities Executives (SFE) simplify the window structure to a SDOF system. The both guides employ large deflection theory to treat the pre-crack behavior of laminated glass. After glass cracks, the window can be idealized as a flexible membrane. The equivalent load-mass factors and the resistance functions are obtained by analytical approach or based on test data. The accuracies of the estimations from these SDOF models differ. Variation was mainly arisen from

different resistance functions and load-mass factors adopted. It is difficult to account for the residual resistance of progressively cracked glass. Instead of using a constant load-mass factor, Morison derived his load-mass factor based on data from two field tests [5]. The load-mass factor was dependent on the pane deflection level. Apart from the above two design guides, ASTM F2248 (in practice with E1300) [8] and UFC 4-010-01 [9] are also facilitated with blast resistant glazing design. ASTM F2248 specifies an equivalent 3-sec design loading to use with ASTM E1300 to determine the thickness of laminated glass windows. Glass failure prediction model with failure probability of 0.008 is used for glass, and the glass pane is designed to 'break safely'. The laminated pane maximum central deflection is calculated using Vallabhan-Wang nonlinear plate method and an equivalent effective pane thickness. UFC 4-010-01 provides no specific analysis guidelines for glass windows to resist blast loads but recommends referring to ASTM F2248. Of all the above approaches, only SFE guide was validated with field testing data on laminated glass windows of two sizes, but the testing results are not publicly accessible. The accuracies of these design guides in estimating the response of laminated glass windows of different dimensions, materials and different blast loading scenarios need to be further checked.

Numerical methods have been being intensively used to simulate the responses of laminated glass windows. Wei et al. [10] developed a 3D finite element model with viscoelastic material model for PVB and elastic model for glass. Hooper et al. [11] built a two stage model (pre-crack and post-crack), by assuming glass cracks instantaneously. The strain-rate-dependent Johnson-Cook

model is commonly adopted to represent the overall behavior of laminated glass in the numerical simulations. Experiments on PVB material over the years show that the strain-rate effect is significant [12, 13]. Under static or quasi-static loading, PVB behaves as a viscoelastic material, whereas under dynamic loading the behavior of PVB is elastoplastic or even brittle. Larcher et al. [2] simulated laminated glass with an elastoplastic material model for PVB using dynamic testing data and elastic material model for glass. The accuracy of 3D finite element model, shell element model, and smear model were compared in simulating the response of laminated glass under different blast loadings. It was concluded that detailed a finite element model with solid element could give the best predictions of laminated glass responses. Recent investigations on the material properties indicated that glass is a very complicated material. On the one hand, the strength of annealed glass varies significantly. Hooper et al. [11] mentioned that testing data gathered in the manuscript of European glazing standard prEn 13474-3 [14] from over 700 ring-on-ring tests on annealed glass vary from 30MPa to 120MPa. The variation was attributed to the existence of surface flaws during manufacturing and servicing. A Weibull distribution is usually used to represent this variation in glass strength [15, 16]. On the other hand, glass material is also strain-rate-dependent. Zhang et al. [17] conducted both static and dynamic tests using a Split Hopkinson Pressure Bar (SHPB) on annealed glass, and concluded that both the compressive and tensile strengths of annealed glass will be amplified under dynamic loading. Under high strain rate, the glass strength can be increased significantly. Peroni et al. [18] conducted SHPB tests on high-strength glass which also showed dynamic strength increment with loading

rate. Based on laboratory testing data on annealed glass, a detailed laminated glass model with strain-rate-dependent properties for both glass and PVB materials was developed [19]. The failure modes of laminated glass under blast pressure, the influencing factors such as glass thickness, PVB thickness, glass strength variation, boundary condition, and also the vulnerability of laminated glass to debris impact were systematically studied [20, 21].

Blast tests on laminated glass windows have been carried out over the years. Kranzer et al. [22] tested 7.52mm laminated glass windows spanning 1.1m × 0.9m in dimension, which were subjected to small-scale charges. Pressure and pane deflection histories were recorded. No global window failure was observed due to the small blast loads. Hooper et al. [11] conducted full-scale field blasting tests on 7.52mm laminated glass fixed to a 1.5m × 1.2m robust frame with silicone sealant. Pane deflections were monitored using a 3D digital image correlation instrument. Glass cracks were widely observed, and glass delamination from PVB interlayer was found at pane corners. Window failures were also found at silicone joint leading to the entire laminated pane flying into the testing cube. Many blast tests on glass windows have also been performed by various organizations, but most testing data are confidential and not accessible to the public. The available testing data provide valuable resources to the study of laminated glass window responses. However, due to complexity of the composite structure and material behavior, simply interpolating the testing data does not always lead to satisfactory predictions. In practice, the design analysis is based on simplified approaches, and sometimes detailed numerical simulations. The accuracy of

these approaches needs to be further verified. Therefore, more tests are deemed necessary with various window sizes, glass thickness, and PVB interlayer thickness to better observe the response and failure modes of laminated glass windows, and also to provide more data to calibrate numerical models and verify the accuracy of the simplified design approaches in predicting the glass window responses to blast loads.

In this study, laboratory tests were firstly conducted using a pendulum impact system. Air bag was placed in front of the laminated glass panel to produce uniform dynamic pressure distribution on the panel. Detailed laminated glass failure process was monitored by a high-speed camera. Pane central deflection and applied pressures were also recorded, and used to check the accuracy of the predictions according to the approaches defined in existing design guides and SDOF analysis. Then full-scale field blasting tests were carried out on laminated glass window of different thickness. Pane deflection histories were recorded with deflection measurement devices. High-speed cameras were used to monitor the deformation and failure of laminated panes and to assist the deflection measurement. The current testing data together with those available in the open literature by other researchers were used to check the accuracy of the predictions according to the design guides, SDOF analysis, and numerical simulations.

2. Laboratory Test

A preliminary investigation was conducted using a pendulum impact system in the laboratory to study the detailed failure process of laminated glass under

lateral dynamic pressure. Four laminated panes of different specifications were tested. The laminated specimens, the pendulum testing system and the experiment procedures are detailed in the following.

2.1 Description of Window Specimen and Testing System Setup

Each laminated glass pane consists of two annealed glass plies laminated with a layer of PVB. The specimens were provided by major Australian window glass supplier, which were freshly manufactured without exposing to weather conditions. The specimens were 670mm × 670mm in dimension with 35mm embedment leaving a 600mm × 600mm clearing surface to be subjected to the uniform pressure. To study the influences of glass and interlayer thicknesses on the response of laminated pane, specimens with glass plies of 3mm, 6mm and PVB interlayer of 0.38mm and 0.76mm were considered. Table 1 lists the specifications of the tested panes.

Pendulum impact testing is a generally adopted method to introduce impact loading to a testing panel [23]. In this study, a traditional pendulum impact device has been modified by inserting an inflated airbag between the testing pane and the impacter. Figure 1a illustrates the pendulum impact system setup for the current test, which consists of a rigid steel rig, a swing impacter with an inclinometer at the hinge, a strike plate, a support frame, an airbag inside a confined frame and data measurement instruments. The steel rig was fixed firmly onto the floor to support the entire system. The impacter weighted 300kg was connected to the end of a 2.8m long steel arm, which in each test was lifted to the desired height and then released to hit the strike plate. It is worth to mention

that after each impact, the impacter was manually held back to avoid rebound causing a second strike. A 35mm thick strike plate was positioned in front of the airbag so as to fully confine the airbag, preventing airbag bursting due to the large impact loads, and to distribute the impact force on the airbag. The airbag was inserted in the confining frame between the strike plate and the specimen. Some pressure was pumped in before the impact to make sure the airbag is in proper contact with the specimen. When the impacter hits the strike plate, it quickly compresses the airbag to generate uniform dynamic pressure acting on the laminated glass specimen. The modified pendulum airbag impact device has been used in previous testing [24, 25]. It was found with the above setup a peak dynamic pressure of 20 to 30kPa (duration about 100ms) can be achieved when the impacter is lifted to 30 degree.

The glass specimen was fully clamped by two clamping frames around all sides (Figure 1b). The clamping frames were firmly fixed in the gap between the confining frame and the supporting frame with eight M10 bolts. Plastic pads slightly thicker than the glass specimens were placed in the gap between the two clamping frames to ensure glass would not be damaged during installation by the clamping forces.

A pressure transducer (Honeywell 24PCD) was inserted inside the airbag to record air pressure applied on the glass specimen. A laser Linear Variable Displacement Transducer (LVDT by Keyence LB72) was elevated to the centre of the glass pane to measure the deflection history at the centre of the specimen. To assist the LVDT tracking pane displacement, a marking dot was glued to glass

pane centre. The pressure and displacement data were captured at a sampling rate of 50 kHz using a National Instrument USB-6363 acquisition system. A high-speed camera (Mikrotron GmbH®) was installed to monitor the failure process of the laminated glass panes. The high-speed images were post-processed using a tracking algorithm to derive the glass deflection histories. The derived glass pane deflection history by high-speed camera was verified with the recorded deflection by LVDT. A 1500W halogen light was installed to provide intensive light for the high speed camera. The framing rate of the high-speed camera was set to 1500fps. A group of strain gauges were glued on the outer glass ply intended to measure the strain of glass ply. However, due to the irregular cracking pattern of glass, no useful data were retrieved.

2.2 Experiment Results

The impacter was lifted and released at an angle of 30°. The pressures recorded by pressure transducer in each test were integrated to derive the impulses. The corresponding peak pressures and impulses together with the maximum central deflections, w_{max}, are listed in Table 1. Detailed observations through high-speed camera images on the laminated pane deformation process, the failed laminated glass pattern, the measured pressure and displacement time histories are given in this section.

2.2.1 Deformation process and failure pattern

Figure 2 to 5 show snapshots of laminated glass pane deformation till failure recorded by the high-speed camera. As shown, for the 6.38mm laminated glass pane (Figure 2), under the uniform pressure from airbag the pane began to

deform. At about 20ms coarse cracks were formed on the outer glass ply. These cracks are confirmed on the outer glass ply because the cracks and the associated shadows on the yellow airbag do not coincide owing to the camera angle. As pane deflection increased, more cracks were developed on the outer glass ply. At 33.3ms the inner glass ply started to crack and broke into numerous small pieces. The cracks on the inner ply are distinguished from those on the outer ply through close examination of the high-speed camera image which reveals that the former are not associated with shadows. The deflection of the cracked laminated pane quickly developed. It reached the peak deflection at about 100ms, and then gradually rebounded. Similar observation can be found on the 6.76mm laminated glass pane (Figure 3) without significant difference except a second peak was observed on pane central deflection after rebound due to a small second impact. It should be noted that in the test, after the first impact, the impacter was stopped by pulling it back manually to avoid repeated impacts. This is not always achieved because of the speed and large mass of the impacter. In the tests of 6.76mm and 12.38mm pane as will be discussed later, a small second impact occurred. This small second impact, however, does not affect the observations of the response and damage of the tested glass panes because they are governed by the first primary impact. The high–speed camera images on the laminated glass with 3mm glass plies show that under lateral pressure, the failure of laminated glass is a gradual process that the outer and inner glass plies crack in steps, and the PVB interlayer retain the cracked glass shards and continue to deform. The inner layer under compressive force breaks into much smaller shards than the

outer layer. As the pane deformation develops the cracked outer glass ply will further break into smaller shards.

High–speed camera images on the laminated panes with 6mm glass plies show a different failure process. As depicted in Figure 4 for the 12.38mm laminated glass, under the airbag pressure, the outer glass ply broke into numerous small splinters with many cracks, instead of few coarse cracks. As pane further deformed, the inner glass ply cracked. Due to the dense cracks on the outer glass layer, it is difficult to distinguish the crack format on the inner layer from the high-speed camera images. A smaller peak deflection was observed as compared to the thinner laminated glass panel. Similar failure process can be observed on the 12.76mm laminated pane in Figure 5. The difference between the laminated panes with 3mm glass plies and 6mm plies can be attributed to the stiffness difference of the two glass panes.

The failure patterns of the tested laminated glass panes are shown in Figure 6a-d. As can be observed, dense glass cracks were formed at the pane centers. These were results of flexural deformation under the uniform pressures. Glass cracks extended radially toward the four corners. Glass around pane corners experienced severe damage especially for the 6.38mm (Figure 6a) and the 6.76mm (Figure 6b) laminated glass panes. PVB rupture was found on the 6.38mm glass at the pane centre (Figure 6e) due to the significant flexural deformation. No interlayer damage was observed on the other laminated panes. Denser cracks were largely observed on the 12.38mm (Figure 6c) and the 12.76mm (Figure 6d) panes. The 12.76mm laminated pane experienced less

severe damage possibly due to the smaller pressure achieved in the impact test as indicated in Table 1.

2.2.2 Quantitative results

The pressure inside the airbag is a key parameter in studying the response of the laminated glass pane. Figure 7 shows the pressure time histories recorded by the pressure transducer. To ensure proper contact between airbag and glass specimen, and uniform distribution of pressure on the glass panel the airbag was inflated with an initial pressure of 2kPa after being inserted into the confining frame. Once impacted and compacted by the strike plate, the air pressure quickly jumped to around 20kPa to 30kPa. The peak pressure was not consistent despite the initial pressure in the airbag and the lifting heights of impacter were kept the same. This is because of the interaction between the tested specimens and the airbag. In general, higher peak pressures were measured on the stiffer panel, i.e., 12.38mm and 12.76mm panes which had smaller deflections. The less deformed panes confined the expansion of the impacted airbag and therefore resulted in higher pressure in the airbag. The air pressure inside the airbag attenuated gradually to ambient after reaching the peak value. The duration of the effective air pressures recorded was about 100ms. It should be noted that this is a lot longer than that from a normal explosion other than in a confined explosion scenario.

The displacements at the pane centers were recorded with laser LVDT and high-speed camera. As shown in Figure 7b, the displacement signal of LVDT oscillated as the tracking point at the specimen centre was not traveling strictly

perpendicularly to the pane. In comparison, the high-speed camera image provides a close enough measurement of glass pane displacement. Because of the variation on LVDT signals, the pane displacement histories monitored and derived from the high-speed camera images are adopted herein. As depicted in Figure 7b for the 6.76mm pane, the laminated glass panel responded quickly under the air pressure and reached a peak deflection of about 32mm. The laminated pane rebounded, after which a second peak deflection was reached because of a second impact. A 10mm residual deflection at the centre of the pane was resulted indicating the plastic deformation of PVB interlayer. The 6.38mm laminated glass pane showed a similar response characteristic under the air pressure (Figure 7a). A maximum central displacement of 29.4mm was reached under the 20.6kPa air pressure, and about 20mm residual displacement was resulted. As shown in the figure, the initial rising parts of the 6.38mm and 6.76mm panes were very similar. However the increase in deflection on the 6.38mm pane became gradual before it reached its maximum deflection. The difference is because of the different damage level of glass plies. As shown in Figure 3-4 and Table 2, the glass plies of the 6.76mm pane experienced more severe damage with more numbers of shattered finer shards under the higher pressure and impulse as compared to the glass of the 6.38mm pane, which experienced relatively smaller pressure loading. The relatively larger pieces of glass shards on the 6.38mm panes were retained by the interlayer and provided larger flexural stiffness than the more severely damaged 6.76mm pane. Since the PVB interlayer has relatively small stiffness as compared to the glass plies, the glass pane flexural rigidity is provided primarily by the glass plies. As damage

develops, the more severely damaged 6.76 mm pane suffered more significant stiffness reduction and therefore deformed faster than the 6.38mm pane. Similarly the more severely shattered 6.76mm pane had less capability of retaining its deformation. Therefore, smaller residual deflection was found on the 6.76mm pane. Similar deflection histories were recorded on the 12.38mm and the 12.76mm laminated glass panes. A maximum central deflection of 7.4mm and 6.5mm were reached respectively. A residual deflection of about 2.3mm was observed on the 12.38mm pane after rebounded from its second peak deflection. In comparison a residual deflection of about 4.5mm was observed on the 12.76mm laminated glass pane. The 12.76mm laminated pane with thicker interlayer displayed a larger residual deflection of 4.5mm than that of the 12.38mm pane with the residual deflection of 2.3mm. As explained above, this is because the higher pressure and impulse applied to the 12.38mm pane caused severer damage to glass plies, which lead to more significant stiffness reduction of the glass pane.

2.3 Analysis and Discussion

The effects of pane configurations, i.e. glass thickness and PVB interlayer thickness, on the responses of laminated glass under uniform impulsive loadings are analyzed. The laboratory test results are compared with the estimations of design standards including ASTM F2248, UFC 3-340-02, and those from analysis of the equivalent SDOF systems by Biggs [26] and Morison [5]. The accuracies of the above models are evaluated through comparisons with the testing results.

2.3.1 Effect of glass thickness

The responses of the four tested laminated glass panes with different glass ply and PVB interlayer thicknesses are summarized in Figure 8. As demonstrated on the deflection histories, the effect of glass ply thickness on the deflection of laminated glass pane is apparent. Under about 20kPa uniform pressure, substituting 3mm glass ply with 6mm ply effectively reduced the maximum pane deflection from around 30mm to below 10mm. This is because of the significant increase in pane flexural stiffness and inertial resistance when using a thicker glass pane. Testing results also indicate that thicker glass ply helps to reduce the residual displacement. The residual displacement reduced from about 20mm for the laminated glass panes with 3mm thick glass plies to below 5mm for those with 6mm glass plies.

2.3.2 Effect of interlayer thickness

The effect of interlayer thickness on pane maximum deflection is not significant. As shown in Figure 8, for the pair of laminated panes with 6mm glass plies, a maximum central deflection of 7.4mm was resulted for the pane with 0.38mm PVB interlayer as compared to the 6.5mm maximum central deflection on the pane with 0.76mm PVB interlayer. Although the PVB interlayer thickness was doubled, the reduction in the maximum deflection was more likely caused by different air pressures applied on the pane as discussed above (30.6kPa for 12.38mm pane vs 23.7kPa for 12.76mm pane). This is because the PVB interlayer is quite flexible and has relatively insignificant contribution to the stiffness of glass panes. As glass has higher density and stiffness than PVB interlayer, the inertial resistance and stiffness of glass pane are governed by the glass plies.

Therefore increasing the thickness of glass plies significantly reduces the deflections of glass pane, whereas increasing the PVB thickness has insignificant effect on glass pane maximum deflection under blast loadings. But as mentioned above, PVB rupture was observed on the 6.38mm pane (at about 5% maximum deflection over span ratio); while no PVB damage was found on the 6.76mm pane with a thicker interlayer and higher maximum deflection. Therefore, it can be concluded that PVB interlayer thickness has no significant influence on the maximum deflection of laminated glass under impulsive loads, but a thicker interlayer improves the rupture resistance of the laminated pane.

2.3.3 Comparison with design standards and SDOF models

The responses of the laboratory tested laminated glass panels under impulsive loadings are compared in this section with predictions from the design standards ASTM F2248, UFC 3-340-02, and SDOF analysis developed by Biggs and the improved SDOF system for laminated glass by Morison.

ASTM F2248 provides design procedures to determine the required thickness of laminated glass to resist specified uniform pressure applied laterally. Glass failure prediction model is adopted in ASTM to determine glass breakage with a failure probability of 0.008. Design charts are available in the ASTM code providing approximate maximum glass pane lateral deflection. Additional procedures are also provided in its appendix to manually estimate pane deflection under specified lateral pressure. The effective thickness of laminated glass is calculated by considering the partial shear resistance from glass and interlayer. Vallabhan-Wang nonlinear analysis is then used to calculate the

maximum pane deflection. Figure 9 shows the estimated pane maximum deflections using ASTM and the testing deflection time histories. Since only the maximum pane deflections can be calculated with ASTM approach, only straight lines instead of pane response histories can be obtained. It can be observed that the maximum deflections determined by the ASTM approach are a lot smaller than those measured in the tests. As summarized in Table 2, the maximum deflections determined by the ASTM approach are generally less than half of the laboratory tested results. The greatly underestimated pane deflections indicate that the ASTM standard overestimates the stiffness of laminated glass and gives very poor estimations on laminated glass deflection when analyzing pane response under impulsive pressure.

UFC 3-340-02 simplifies the laminated glass window into a SDOF system as illustrated in Figure 10a. Large deformation theory is used to analyze the pre-crack behavior of laminated glass. The thickness of the laminated pane is equivalent to a monolithic pane by considering the ratio of Young's modulus between glass and PVB material. When glass cracks, the laminated pane is then idealized to a PVB membrane with distributed mass representing the cracked glass. According to Cormie [27], the resistance function is determined in two phases: pre-crack and post-crack. Moore's study [28] on monolithic pane response to uniform pressure gives the pre-crack resistance function. Static membrane analysis under a uniformly distributed load yields a polynomial load-deflection relationship for the cracked laminated glass pane (as shown in Figure 10b). Variation is found on the equivalent load-mass factor used in UFC 3-340-02

(K_{LM}=0.61) and that of classic theory by Biggs (K_{LM}=0.63). To check the influence of this variation, SDOF model with load-mass factor by Biggs [26] is also derived and analyzed. As shown in Figure 9 and Table 2, the UFC guide with SDOF models gives better estimations of laminated glass responses than those using ASTM. UFC slightly underestimates the maximum deflections of the laminated glass panes in the current tests. The variations between the UFC estimation and that from Biggs are marginal. The SDOF models with Biggs' equivalent coefficients predict a little lower pane deflection because the larger K_{LM} adopted. Closely examining the tested pane central displacement histories and those from UFC and the Biggs' SDOF models, it can be found that the SDOF models are relatively flexible. For instance, in testing the deflection of the 6.38mm laminated pane quickly increased to 31.9mm at around 100ms, and then gradually decreased. In comparison, the deflection of the laminated glass pane predicted by the SDOF models increases much slowly. The maximum deflection is reached at about 150ms. Similar behaviors can be observed in other groups of tests. This difference could be due to the boundary conditions. Although fixed boundaries are assumed in selecting K_{LM} for both the UFC guide and the Biggs' classic model, in determining the pre-crack resistance function, UFC guide treats the laminated glass pane as simply supported on all four sides to account for silicone squeezed in the gap between glazing and steel frame. In the UFC 3-340-02 for glazing window design, only simply supported boundary condition is assumed for all the cases. In contrast, laminated glass specimens were fully clamped using two steel frames without any silicone in the test. Considering the size of the pane, i.e. 600mm by 600mm and the embedment depth of 35mm on all sides, the tested

panes were firmly fixed, which led them to respond faster to the applied pressure as compared to a pane with simply supported conditions. Recent field blast tests conducted by Zhang et al. [29] also found that with simply supported boundary condition as assumed in UFC 3-340-02, the response of fully clamped monolithic tempered glass windows could be greatly misestimated [29]. In the current test, after glass cracks along its boundaries, the panes lost flexural resistance at supports. The boundary conditions of the tested panes became similar to those of the SDOF models derived with simply supported conditions. As a result the slopes of pane during rebound are quite close to that of the SDOF models as shown in Figure 9, indicating similar stiffness of the pane.

The underestimation of laminated glass pane deflections in the UFC standard and the classic SDOF model could be attributed to two possible reasons: firstly, the misalignment in load-mass factor because of the different boundary conditions as discussed above. The above comparison between testing data, UFC and classic SDOF model indicates that using a smaller K_{LM} factor leads to a closer prediction of the testing data. High-speed images on the failure process of laminated glass showed that glass plies cracked progressively. Glass plies gradually lost their resistance as cracks developed into finer splinters. In addition, the static resistance function adopted in deriving the equivalent SDOF model is not exactly accurate. Previous resistance function uses a polynomial relation to represent the laminated glass post-crack behavior based on viscoelastic property of PVB. Recent dynamic test on PVB material properties shows that PVB behaves as an elastoplastic material under short time loading. This leads to a resistance

function that does not increase with deformation but deforms significantly with a small increment in pressure owing to plastic flow. SDOF model with Morison's modified static resistance function is also developed and used to analyze the laminated glass responses in the current tests. Morison's SDOF model for the laminated glass pane also yields very similar results. As shown in Table 2 and Figure 9, the estimated pane responses using Morison's model almost replicated that from Biggs' SDOF model. The two SDOF models give similar predictions because all the glass panels considered in the current tests experienced only relatively insignificant deflections under the pendulum impacts, and the resistance functions as shown in Figure 10b for the 6.76mm laminated glass for the two models are almost the same when the deflection is smaller than 50mm.

The above analysis and comparisons with pendulum testing results on laminated glass window found that ASTM F2248 gives very poor estimation on window response under impulsive loading, but UFC 3-340-02 provides accurate estimations. The error in the derived pane responses using UFC code, Biggs' classic SDOF model and the Morison's modified SDOF model with respect to the testing data are small under the current test situation, indicating the laminated glass window responses under such impact loads can be reliably predicted by using either one of these methods. However, the accuracy of these methods in predicting laminated window responses under large explosion loads needs also be examined because as shown in Figure 10b, the resistance functions in UFC and Morison's model deviate from each other when the deflection is large, which would lead to different response predictions.

3. Full-scale Field Blast Test

The above comparisons demonstrated that the SDOF analysis-based methods yield reliable predictions of laminated glass window responses to uniformly distributed impulsive loads when the deflection of the window panel is relatively small. Glass windows might be subjected to blast loads with large deflections. The reliability of these methods in predicting the window responses to blast loads is also evaluated in this study.

Full-scale field blast tests on laminated glass windows were carried out and described in this section. The testing results are used to evaluate the accuracy of the above design and analysis methods when the deflection of window structure is large. Window responses under air blast pressure and pressure-impulse analysis are checked in details. Accuracy of the predominant numerical models of laminated glass and UK glazing hazard design guide by SFE in predicting the window responses are also included in the evaluation.

3.1 Test Setup and Results

3.1.1 Testing field

Figure 11 sketches the site setup of the field blasting test. A 3.4m wide by 3.2m long by 2.0m tall reinforced concrete (RC) block with deep rooted independent footings was constructed to support the window specimens. The RC block is comprised of two individual rooms. The back wall of the block was left open for high-speed cameras to monitor the failure process of the windows. Two openings were pre-set on the front wall for the 1.5m by 1.2m windows. The laminated glass windows were fully clamped with steel frames. 20mm thick inner

frames were firstly fixed onto the RC block with M24 bolts. The laminated glass specimens were then held in place, which were fastened by four pieces of 10mm thick steel strips (as outer window frame) using M12 bolts. Similar to the practice as shown in Figure 1b, plastic strips were placed in the gap between the inner and outer window frame to avoid damaging glass specimens when fasten the bolts.

3.1.2 Testing scenario and data acquisition system

Five laminated glass specimens were tested in three blast trials. Table 3 summarizes the laminated glass pane and charge specifications. In Test 1, two laminated panes with 3mm glass plies were tested in pair to evaluate the influence of PVB interlayer thickness (1.52mm PVB vs 2.28mm). A laminated pane with 3mm thick glass ply was tested with another pane with 6mm glass ply to check glass thickness effect in Test 2. A 7.52mm laminated glass specimen (3mm glass, 1.52mm PVB, and 3mm glass) was tested in Test 3 with a monolithic tempered glass. The response of the monolithic pane is irrelevant with this paper. Therefore it is not discussed here. More details about the study based on the testing results on monolithic glass windows are presented in reference [29, 30]. 10kg TNT explosives were positioned at various stand-off distances as listed in Table 3, and detonated in front of the window specimens.

A pressure sensor was installed on the front wall between the two glass specimens. Two mechanical Linear Variable Displacement Transducers (LVDT) were used to measure the central displacements of the glass specimens. The pressure and displacement transducers were wired to an amplifier, and the

testing data were captured with National Instrument portable data acquisition system. The sampling frequency was set to be 500 kHz. The failure process of the laminated panes was monitored by two high-speed cameras (Fastcam SA3 Photron®). Heavy steel bunkers were used to protect the high-speed cameras from potential glass fragments. The camera lens was set with widest opening, and the exposure time was set to the smallest duration to balance aperture. The high-speed cameras were filming at 2000Hz owing to the restriction of the camera and lens configuration. The high–speed camera imaging and the data acquisition were triggered by external wires which were glued onto the charge.

3.1.3 Pressure time history

Cylindrical TNT explosives were casted with a central perforation of 5cm diameter for high explosive RDX as the booster charge. The booster was primed with electric detonators inserted into the axis of the booster charge (As depicted in Figure 11b). Detonation of explosives results in a rapid release of energy. Figure 12 shows the pressure time histories recorded by the pressure transducer. It can be observed that blast waves arrived at the front wall of the testing block some time after detonation. The air pressure acting on the front wall rose almost instantaneously to a peak, and then attenuated quickly back to ambient. Significant negative pressures were found for all the three blast tests. Apparent fluctuation was recorded on the pressure time history in Test 3, which was likely to be resulted from the fracture of the monolithic glass pane next to the pressure sensor.

The measured reflected pressures are integrated along time to derive the reflected impulses. The computed reflected impulses and recorded reflected pressures are listed in Table 4 in comparison with the predictions using UFC 3-340-02. The experimentally measured reflected pressures are consistently higher than those estimated with UFC 3-340-02. The reflected positive impulses measured in the current tests are also larger than those by UFC code. This could be attributed to charge shape [31] or the core booster charge. More variations were found on the negative impulses, which were probably due to the testing site condition, the size and shape of the RC block.

3.1.4 Deformation process and failure pattern

The deformation process of each laminated glass pane when subjected to air blast wave was monitored by high-speed cameras. Figure 13 shows the snapshots of high–speed camera images of pane 2-1-1 and 2-1-2. As shown in Figure 13a, air blast wave arrived at the testing pane at about 15ms after detonation. The glass cracks were formed 2ms later on the 7.52mm laminated glass as pane deformed under air pressure. The glass broke severely with very dense cracks along the boundaries and a few coarse cracks at pane centre. Significant deformation pulled the cracked laminated pane out of the frame along two vertical boundaries. At about 50ms, the pane was totally dragged out of the frame during rebound.

In contrast, the laminated pane with thicker glass plies (6mm thick) responded very differently under the same blast loading as shown in Figure 13b. The glass cracked at a slightly earlier stage (about 1ms after blast wave came into

effect). This was because the thicker glass pane 2-1-2 had larger flexural stiffness than pane 2-1-1. It responded faster under the blast load. The ultimate tensile strength of the thicker glass was reached at an earlier stage and at a lower deflection level. Cracks extended and numerous glass shards were formed but held by the PVB interlayer. The cracked laminated glass pane reached a maximum deflection at about 21ms and rebounded without being pulled out from the window frame. The cracked laminated pane was retained within the window frame.

From the high-speed camera images on the failure processes of the laminated glass panes, glass cracks and significant PVB interlayer deformation were widely found which were very much similar to the observation in the laboratory tests. However, the failure patterns of the laminated glass panes in the field blast tests differed from those in the pendulum tests. Figure 14 provides the images of the tested laminated glass panes. As can be observed in Figure 14a, d, and e, the glass plies of the laminated panes were badly damaged. All these panes eventually deformed towards outside of the testing cube indicating plastic deformation of PVB interlayer and the suction of negative pressure. The 7.52mm glass pane shown in Figure 14a experienced severer damage than the other 7.52mm pane shown in Figure 14e. The difference was attributed to the larger blast pressure applied to the former pane in Test 1. Pane 1-1-2 also experienced severe glass cracking damage. In addition, the cracked laminated pane was partially pulled out of the window frame along its left and bottom boundaries (Figure 14b). The 7.52mm laminated glass pane (pane 2-1-1) experienced the

worst damage. The pane was totally pulled out of the frame by the overwhelming negative pressure (as shown in Figure 13a), and fell out of the window frame. In comparison, due to the nature of the pendulum impact test, no negative pressure could be generated by the airbag. All the cracked glass panes were pushed in the impact direction, and none of these panes ended up deforming towards the airbag. The smaller window span and relatively lower pressure levels in the pendulum test resulted in smaller pane central deflections. None of the tested laminated panes failed at its boundary and were pulled out of the frame.

3.1.5 Displacement history

Two mechanical LVDT transducers were used to record the central displacement histories of the laminated glass panes. The probes of the transducers were glued to the central points of the laminated glass specimens. They followed the laminated pane movements as they deflected inwards the room and rebounded. Debonding between the probes and the cracked glass occurred soon after the panes started to rebound. Nevertheless, the maximum central deflections were recorded for all the panes involved in the current tests.

The recorded deflection time histories are presented in Figure 12. The time axis is aligned with the aid of high-speed camera images so that the deflections started only when the blast waves came into effect. The deflection histories were abridged at the instant when probes debonded from the laminated panes. As demonstrated in Figure 12a, under the air blast weave the laminated glass pane deformed gradually at the beginning due to the flexural rigidity of the un-cracked laminated glass pane. The deflection increased quickly as the laminated pane lost

flexural stiffness after glass plies cracked. The maximum deflections of 275mm and 280mm were recorded at about 15ms for pane 1-1-1 and 1-1-2 respectively, after which the panes began to rebound under the negative pressure. The other two 7.52mm laminated panes (2-1-1 and 3-1-1) responded similarly (shown in Figure 12b and c) as those above. Under the blast pressure, both the 7.52mm laminated panes experienced the maximum deflections of 326mm and 264mm, respectively and then rebounded. The difference in peak deflection was mainly because of the magnitudes of blast loading. The 13.52mm laminated pane (2-1-2) also experienced similar response, but it responded faster due to larger flexural rigidity with a smaller maximum central deflection of 220mm. The maximum central deflections together with the associated positive reflected pressures and impulses are summarized in Table 5.

3.2 Analysis and Discussion

In this section, the effects of glass ply thickness and PVB interlayer thickness on responses of laminated glass windows subjected to blast loading are analyzed and discussed. The measured central deflection histories of the 7.52mm laminated panes are then compared with the estimated pane responses according to the design guides UFC and ASTM, as well as the classic and Morison's modified SDOF models. The accuracies of these methods are evaluated. The current testing data, together with those obtained by other researchers are also used to check the accuracy of the P-I diagrams generated by the above methods and by some recent numerical models.

3.2.1 Glass thickness influence

To investigate the influence of glass ply thickness on the window response, a 7.52mm laminated pane (2-1-1) with 3mm thick glass ply and a 13.52mm pane (2-1-2) with 6mm glass ply were tested in pair with 10kg TNT explosive detonated at 9m stand-off distance. As shown on the recorded central deflection time histories (Figure 12b), under approximately the same blast load the thicker pane responded quicker due to its higher flexural stiffness. A peak deflection of 220mm was recorded at about 7ms after blast wave arrived. In comparison, the thinner pane deformed slower but a larger maximum deflection of 326mm was induced at around 15ms. The difference was because the thicker glass pane had higher flexural stiffness and larger inertial resistance. Under the same blast loading it deformed less in comparison with a thinner glass pane. Figure 14c and d show that the tested 13.52mm laminated pane stayed in the window frame, while the 7.52mm pane was totally pulled out of the frame because of the significant deflection. The failure found on the thinner glass pane was likely due to the more significant pane deformation and central deflection, which led to the pulling-out failure around its boundaries. The comparison of the recorded deflection time histories and failure images indicates that thicker glass panes have higher blast loading-resistant capacities.

3.2.2 Interlayer thickness

The effect of interlayer thickness on the blast-resistant capacity was examined by testing 3mm glass plies laminated by a 1.52mm (pane 1-1-1) and a 2.28mm PVB interlayer (pane 1-1-2). The deflection time histories (Figure 12a and c) show that the laminated pane with 1.52mm interlayer responded similarly to the one

with 2.28mm interlayer. Despite having a thicker interlayer, a slightly larger maximum deflection (280mm) was recorded on the 8.28mm laminated glass pane. This resulted in the cracked laminated pane being partial pulled-out of the window boundary as shown in Figure 14b.

Careful examination of the tested laminated pane with 1.52mm interlayer found some PVB ruptures (Figure 15). A maximum deflection of 275mm was measured on this laminated pane. In comparison, a maximum deflection of 264mm was measured on pane 3-1-1, on which no PVB tearing was observed. If the maximum deflections at pane centers are normalized by the pane width to derive the deflection over span ratio for these two panes, it appears that PVB rupture initiated at about 23% (275mm/1200mm for pane 1-1-1), whereas no PVB damage was found when deflection over span ratio was 22% (264mm/1200mm for pane 3-1-1). However, for pane 1-1-2 with PVB thickness of 2.28mm, although the maximum deflection of 280mm was slightly larger than that of pane 1-1-1, and the deflection over span ratio was slightly more than 23%, no interlayer rupture was observed, demonstrating that a thicker interlayer helps to improve the anti-tearing capacity of the laminated glass panel. Through the above comparison it can be found that a thicker PVB interlayer does not result in lower pane deflection as its enhancement on pane stiffness and inertial resistance is insignificant, but it reduces the PVB rupture potential.

3.2.3 Comparison with design guides and SDOF methods

Responses of the 7.52mm laminated glass comprising 3mm glass plies and 1.52mm PVB interlayer are predicted by using the procedures specified in the

design guides and the equivalent SDOF analysis. The accuracy of the UFC and ASTM procedures, classic SDOF model and Morison's modified SDOF model are evaluated through comparisons of the predicted and the field testing data. Three tested 7.52mm laminated glass panes (1-1-1, 2-1-1, and 3-1-1) with different loading conditions are considered.

As mentioned in the above sections, ASTM F2248 estimates the maximum deflection of laminated glass pane using nonlinear plate theory. The magnitude of pane deflection depends on the level of applied pressure and the equivalent effective thickness of the laminated pane. As shown in Figure 16and Table 6, similar to the comparisons carried out in the pendulum test, the maximum deflections estimated by ASTM F2248 are a lot lower than the measured deflections for all the three panes involved in the current field blast tests. For instance, ASTM standard estimates a maximum deflection of 72mm for pane 1-1-1 under 121kPa reflected pressure, while in the field test a maximum deflection of over 275mm was measured at pane centre. For pane 3-1-1 which was subjected to 82kPa reflected pressure, a maximum deflection of 264mm was recorded in the field test. In comparison, the maximum deflection estimated by ASTM was only 62mm. The comparison indicates that ASTM standard greatly underestimates the responses of laminated glass under blast loadings.

The equivalent SDOF model of laminated glass with the tested configuration was derived following UFC 3-340-02. A static resistance function as suggested by Cormie [27] is generated for 1.5m by 1.2m laminated glass window (Figure 17). A constant load-mass factor of 0.65 was adopted according to the UFC code (Figure

18. As depicted in Figure 16, the UFC guide better predicts the behavior of the laminated glass windows than ASTM code, but the maximum pane deflection was still underestimated. For instance, when the laminated glass window was subjected to 121kPa peak pressure and 395kPa-ms impulse blast loading, the UFC guide well predicts the initial response. A maximum deflection of 181mm was predicted at about 14ms and then rebounded, whereas in the field test the laminated pane continued to deform to about 275mm before rebounding. A variation of about -34% was found between the predicted maximum deflection and that measured in the field blasting test. Likewise, the UFC guide underestimates the maximum deflections of the laminated pane by 32% and 24%, respectively for pane 2-1-1 and 3-1-1.

Using the same resistance function for the classic SDOF model, very similar responses were derived for these three laminated panes (Figure 16). Slightly smaller maximum deflections were calculated by the Bigg's classic SDOF model as compared to those predicted by UFC guide. This is because of the difference in load-mass factors (K_{LM}=0.69 by Biggs [26]). With slightly smaller load-mass factor adopted, marginally higher and closer predictions were resulted by using the classic SDOF model in comparison with the field measured pane deflections. Basically, both the classic method and UFC 3-340-02 use SDOF model to simulate the response of laminated glass pane under blast loading. Since identical static resistance function is adopted, it is only a matter of which load-mass factor better represents the behavior of glass pane in the real test. The above comparison indicates, when subjected to blast loading, the laminated pane

experiences severe damage with large deflection. A lower load-mass factor better represents the situation of the cracked laminated pane. Therefore, the classic SDOF model with a smaller load-mass factor gives a slightly closer prediction.

Very different window responses were derived with Morison's modified SDOF model. As can be found in Figure 16, Morison's model predicts larger laminated pane responses than those measured in the tests. For example, under the recorded blast pressure in Test 1, the modified SDOF model predicts a peak central deflection of 310mm, which is 13% larger than 275mm measured in the test. The difference is primarily because of the change in resistance function. As can be observed in Figure 17, after glass plies break, a polynomial relationship between pane resistance and central deflection is assumed in the model by Cormie. In contrast, based on recent dynamic material testing results on PVB, Morison modified the resistance function that the laminated pane would not provide unlimited resistance to the applied pressure; instead it exhibits finite resistance with significant deflection owing to the large ductility of PVB. In addition, based on observation from field blasting tests, Morison derived a variable load-mass factor, which was related with pane deflection as shown in Figure 18. The gradual fracturing process of glass plies was considered in deriving this deflection dependent load-mass factor. This modified model gives better predictions of the glass window responses measured in the tests as compared to the predictions based on the resistance function proposed by Cormie, but it consistently over-predicts the glass window deflections as shown in Figure 16 and Table 6. For pane 2-1-1 and 3-1-1, Morison's model gives 27% and 39% higher

estimations on the laminated pane deflection respectively. The overestimation of pane response in Morison's model can also be attributed to the inaccurate resistance function, especially at high strain rate. Since Morison's model relates pane stiffness with glass damage, the accuracy of prediction also depends on the damage level of the glass plies. For example, the glass plies of pane 3-1-1 (Figure 14e) were not as badly shattered as the glass plies of panes 1-1-1 (Figure 14a). The glass plies of pane 3-1-1 were largely intact especially near the upper window frame and in the pane central region. The less shattered glass pane had large stiffness and resulted in lower deflection. Through the above comparison it can be found that with modified resistance function and load-mass factor, Morison's model gives more conservative prediction with higher pane deflection. The accuracy of prediction using Morison's model heavily depends on the glass damage and fracture level.

3.2.4 Pressure impulse analysis

The current testing data are also used to evaluate the accuracy of pressure-impulse (P-I) diagrams derived using different methods as shown in Figure 19. Previous blast testing results reported by Hooper et al. [11] on 7.52mm laminated glass window of 1.5m long by 1.2m wide are also included for comparison. These testing data are compared with the P-I diagrams provided by Cormie et al. [27] based on SDOF model analysis, P-I diagrams derived by Hooper et al. [11], and Zhang et al. [21] through numerical simulations. In deriving the P-I diagrams, Cormie et al. [27] considered two failure criteria, i.e. glass crack and PVB interlayer failure. For comparison, the blast resistant capacity of 7.52mm

laminated glass of 1.5m × 1.2m in dimension is also derived using ASTM F2248, and according to the Glazing Design Guide by SFE facilitates. It should be noted that the P-I diagrams of SFE not only distinguish glass crack and interlayer failure, but also consider the effect of window frame enhancement, which supposedly give better and more comprehensive predictions of the blast resistant capacities of the laminated glass window.

It should be noted that in generating the P-I diagrams, glass crack threshold is considered in SFE, Cormie et al.'s SDOF model, and Hooper et al.'s numerical model. In the calculations based on the SDOF model according to the SFE Guide, a static resistance function is used, which includes glass pre-crack phase and post-crack phase (polynomial resistance-deflection relationship). Considering the effect of silicone squeezed into the gap between window frame and glass panel, a load-mass factor of k_{LM}=0.71 is taken by treating the window as a two-way slab simply supported on four sides under uniform pressure. Elastic response is assumed since the deflected shape in the regime is closest to the shape of the deflected membrane. As shown the P-I diagrams according to SFE and Cormie et al.'s approaches overlap with each other indicating their consistency. The pressure and impulse asymptotes from the above two approaches are both higher than those in the Hooper et al.'s numerical model, which according to Hooper et al. is attributed to the inaccurate assumption of uniformly distributed pressure throughout of the pane. As a result, Hooper et al. adopted a much lower impulse asymptote, implying that when subjected to a close-in explosion, glass ply will crack at a much lower impulse around the central region of the glass

pane. As can be noted in Figure 19, all the test data, including those obtained by Hooper et al. lay in the upper right region of the P-I diagrams constructed by the equivalent SDOF approaches, indicating those SDOF methods underestimate the blast resistant capacities of the windows. However, as can be noticed, the P-I diagrams developed by numerical simulations in Hooper et al. [11] and Zhang et al. [21] slightly overestimate the blast loading resistance capacities of the window. Since no evaluation could be made to the above methods about glass crack threshold, focus is therefore placed on the region defining interlayer and overall pane failure. As shown, the predictions of ASTM and SFE for normally fixed windows are quite close in the quasi-static region, indicating these two methods yield similar predictions when the response is governed primarily by flexural responses of the window panel. In the current test, none of the 7.52mm laminated panes generated any glass debris that flied directly into the room. However, pane 2-1-1 was pulled out of the window frame during rebound, which left no residual protection capability against any following threat. Therefore, this pane is judged as failed in the test. Similarly, among the four tested windows by Hooper et al., one laminated pane was pushed out of the frame and flied directly into the room, which is treated as failed. The open blocks in Figure 19 stand for the laminated glass window survived the blast loading, while the solid blocks mean complete window failure, related to the pulling out of the window panel from the support in both tests as described above. In the SFE's guide with enhanced fixed frame and Cormie et al.'s SDOF model, failure is defined by PVB tearing. For the tested window specimens, both approaches defined the PVB tearing to occur when the central deflection reaches 200mm for the 1.2m wide

window, i.e., 17% of deflection over span ratio. As shown, both of these methods with the failure definition according to the PVB tearing underestimate window capacities. On the other hand, the numerical models by Zhang et al. and Hooper et al. both overestimate window capacity. The failure of the laminated glass windows in Hooper et al.'s model is defined by the in-plane principal strain. When the in-plane principal strain reaches 20% after glass cracks, PVB is assumed to be ruptured. In Zhang et al.'s simulation, the laminated glass is assumed to be fully fixed along its boundaries, and the failure of the pane is determined by the ultimate tensile and shear strength of PVB interlayer, namely the tearing of PVB at ultimate strength. Comparison with field testing data shows that the failure criterion based on PVB tearing is not necessarily accurate and sufficient. In the tests carried out in the present study, pane 2-1-1 failed by being pulled out of its frame during rebound, instead of PVB rupture. Similarly in the tests conducted by Hooper et al., complete failure occurred because the window was pulled out of the support and pushed into the room. The possible pull-out failure of the glass pane from its support is not considered in the two numerical models, therefore they over predict the glass window capacities.

The above comparisons indicate that P-I diagrams developed based on equivalent SDOF analysis in general underestimate the blast resistant capacities of laminated glass windows. Numerical simulations give more accurate predictions of the P-I diagrams, however, the possible pulling out failure of the window panel from its support should also be considered in the simulations.

4. Conclusion

In this study, experiments were carried out to investigate the response and blast resistant capacity of laminated glass windows. Both laboratory and field blasting tests were conducted to evaluate the window responses to uniform impact and blast loads. The failure process of the laminated glass panels were monitored by high-speed cameras. The applied impact and blast pressure, as well as the dynamic response of the window specimens were measured in the tests. It was observed that the failure of laminated glass was a progressive process. The outer glass ply, the inner glass ply cracked and the PVB interlayer ruptured in turn. The cracks on the glass plies also grew dense as pane deforms. The recorded pane central deflection and the pressure histories were used to evaluate the accuracy of design standards and equivalent SDOF analysis. It was found that ASTM standard underestimates the laminated glass responses. UFC guide and the other SDOF-based approaches give reliable predictions of glass window responses when the deflection level is relatively small. Under blast loading with large panel deflection, the accuracy of the equivalent SDOF analysis varies. Most commonly used SDOF models underestimate the glass panel responses, while the model by Morison with modified resistance function considering the low resistance and high ductility properties of PVB material and deflection dependent load-mass factor yields better predictions but overestimates the responses. The current and available testing data obtained by other researchers were also compared with the P-I diagrams suggested by others or developed based on various approaches. It was found that P-I diagrams developed from equivalent SODF analysis in general underestimate the blast resistant capacities of the laminated glass windows.

Numerical simulations can yield more accurate P-I diagrams but pulling out failure of the glass pane from its support should be considered in the simulations

Acknowledgement

The authors would like to thank Australian Research Council for financial support. Support from the State Key Laboratory of Science and Technology of Beijing Institute of Technology with its collaborative research scheme under project number KFJJ11-3 is also acknowledged. The first author would also like to thank the University of Western Australia for providing Ad Hoc scholarship.

Reference

[1] Lin LH, Hinman E, Stone HF, Roberts AM. Survey of Window Retrofit Solutions for Blast Mitigation. Journal of Performance of Constructed Facilities. 2004;18:86-94.
[2] Larcher M, Solomos G, Casadei F, Gebbeken N. Experimental and numerical investigations of laminated glass subjected to blast loading. International Journal of Impact Engineering. 2012;39:42-50.
[3] Wei J, Shetty MS, Dharani LR. Stress characteristics of a laminated architectural glazing subjected to blast loading. Computers & Structures. 2006;84:699-707.
[4] Duser AV, Jagota A, Bennison SJ. Analysis of glass/polyvinyl butyral laminates subjected to uniform pressure. Journal of engineering mechanics. 1999;125:435-42.
[5] Morison C. The resistance of laminated glass to blast pressure loading and the coefficients for single degree of freedom analysis of laminated glass. PhD thesis. 2010;Cranfield University.
[6] UFC 3-340-02. Structures to Resist the Effects of Accidental Explosions. UFC 3-340-02, Department of Defense, United States of America, 2008.
[7] Security Facilities Executive Special Services Group - Explosion Protection. Glazing Hazard Guide. Cabinet Office, London, 1997.
[8] ASTM F2248-09. Standard Practice for Specifying an Equivalent 3-second Duration Design Loading for Blast Resistant Glazing Fabricated with Laminated Glass. West Conshohocken, PA, 2009.
[9] Unified Facilities Criteria DoD Minimum Antiterrorism Standards for Buildings. Washington D.C., USA, UFC 4-010-01, 2003.
[10] Wei J, Dharani LR. Response of laminated architectural glazing subjected to blast loading. International Journal of Impact Engineering. 2006;32:2032-47.
[11] Hooper PA, Sukhram RAM, Blackman BRK, Dear JP. On the blast resistance of laminated glass. International Journal of Solids and Structures. 2012;49:899-918.
[12] Bennison S, Sloan J, Kistunas D, Buehler P, Amos T, Smith C. Laminated glass for blast mitigation: Role of interlayer properties. Glass Processing Days. Tampere, Finland2005.
[13] Iwasaki R, Sato C, Latailladeand J, Viot P. Experimental study on the interface fracture toughness of PVB (polyvinyl butyral)/glass at high strain rates. International Journal of Crashworthiness. 2007;12:293-8.
[14] prEn 13474-3. Glass in Buildings - Determination of the Strength of Glass Panes. Part 3: General Method of Calculation and Determination of Strength of Glass by Testing. British Standards Institute. London,

[15]Overend M, Parke G, Buhagiar D. Predicting Failure in Glass—A General Crack Growth Model. Journal of Structural Engineering. 2007;133:1146-55.
[16]Beason WL, Morgan JR. Glass Failure Prediction Model. Journal of Structural Engineering. 1984;110:197-212.
[17]Zhang X, Zou Y, Hao H, Li X, Ma G, Liu K. Laboratory Test on Dynamic Material Properties of Annealed Float Glass. International Journal of Protective Structures. 2012;3:407-30.
[18]Peroni M, Solomos G, Pizzinato V, Larcher M. Experimental Investigation of High Strain-Rate Behaviour of Glass. Applied Mechanics and Materials. 2011;82:63-8.
[19]Zhang X, Hao H. Dynamic Material Model of Annealed Soda-lime Glass under review with International Journal of Impact Engineering. 2014.
[20]Zhang X, Hao H, Ma G. Laboratory test and numerical simulation of laminated glass window vulnerability to debris impact. International Journal of Impact Engineering. 2013;55:49-62.
[21]Zhang X, Hao H, Ma G. Parametric study of laminated glass window response to blast loads. Engineering Structures. 2013;56:1707-17.
[22]Kranzer C, Gürke G, Mayrhofer C. Testing of Bomb Resistant Glazing Systems– Experimental Investigation of the Time Dependent Deflection of Blast Loaded 7.5 mm Laminated Glass. Proceedings of Glass Processing Days. Tampere, Finland2005.
[23]ASTM D3420-08a. Standard Test Method for Pendulum Impact Resistance of Plastic Film. West Conshohocken, PA,
[24]Mutalib AA, Sivapatham S, Hao H. Experimental investigation of CFRP strengthened RC slabs with anchors under impact loading. Proceedings of the 8th International Conference on Shock and Impact Loads on Structures2009. p. 457-65.
[25]Chen W, Hao H. Experimental investigations and numerical simulations of multi-arch double-layered panels under uniform impulsive loadings. International Journal of Impact Engineering. 2014;63:140-57.
[26]Biggs JM. Introduction to structural dynamics: New York; 1964.
[27]Cormie D, Mays, G., Smith, P. Blast Effects on Buildings. Heron Quay, London: Thomas Telford Publications; 2009.
[28]Moore DM. Proposed method for determining the thickness of glass in solar collector panels. NASA STI/Recon Technical Report N. 1980;80:24755.
[29]Zhang X, Hao H, Wang Z. Experimental Investigation on Monolithic Tempered Glass Window Response to Blast Loads. Manuscript. 2014.
[30]Zhang X, Hao H, Wang Z. Experimental investigation of monolithic tempered glass fragment characteristics subjected to blast loads. Engineering Structures. 2014;75:259-75.
[31]Wu C, Oehlers DJ, Rebentrost M, Leach J, Whittaker AS. Blast testing of ultra-high performance fibre and FRP-retrofitted concrete slabs. Engineering Structures. 2009;31:2060-9.

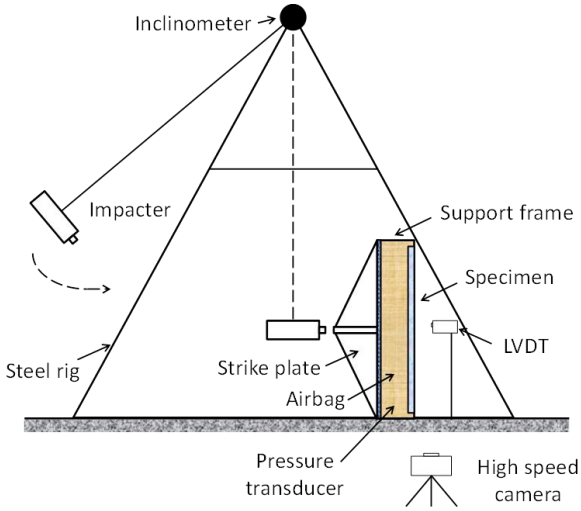

a) Schematic view of the pendulum impact system

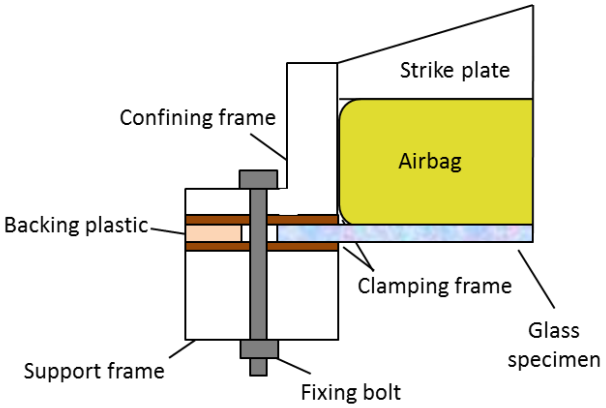

b) Schematic glass fixture

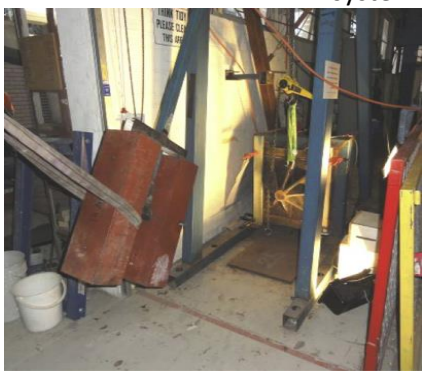

c) Ready-to-go pendulum impact test

d) Impacter, strike plate, confining frame, and support frame

e) Laminated glass specimen setup in frame with LVDT

Figure 1 Pendulum test setup

0ms impacter struck on airbag

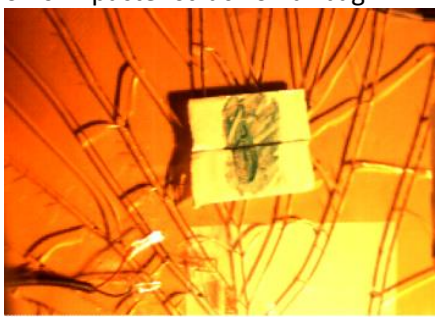

20ms outer glass ply cracked

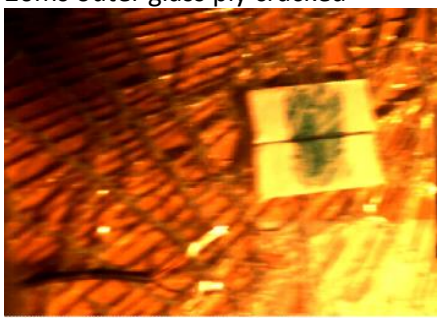

33.3ms inner glass ply cracked

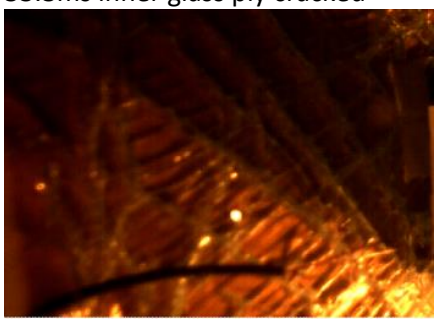

100ms maximum deflection

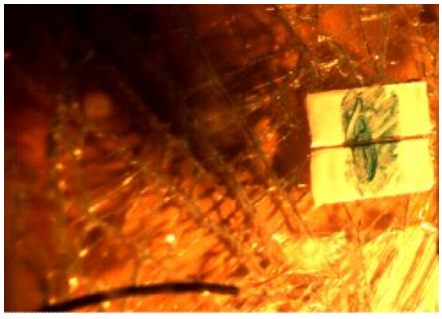

206.7ms rebounded

Figure 2 High-speed camera snapshots of 6.38mm laminated pane

0ms impacter striked on airbag

6.7ms outer glass ply cracked

20ms innter glass ply cracked

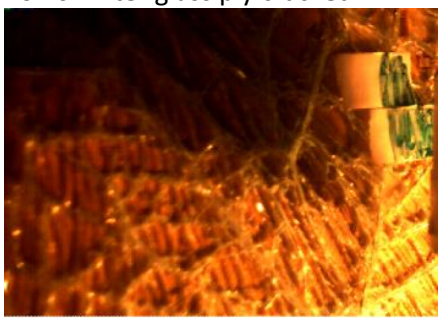

73.3ms maximum deflection

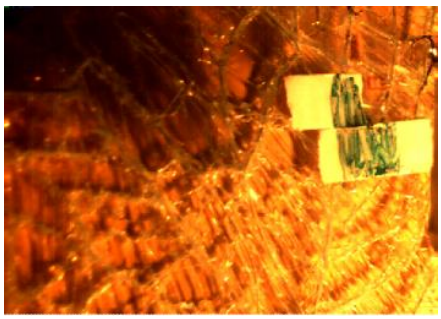

213.3ms rebounded

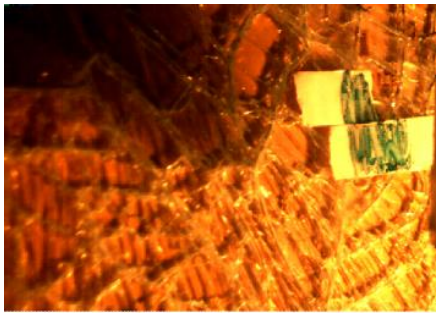

286.7ms 2nd peak deflection

Figure 3 High-speed camera snapshots of 6.76mm laminated pane

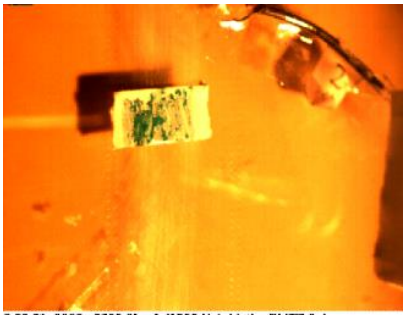

0ms impacter striked on airbag

33.3ms out glass ply cracked

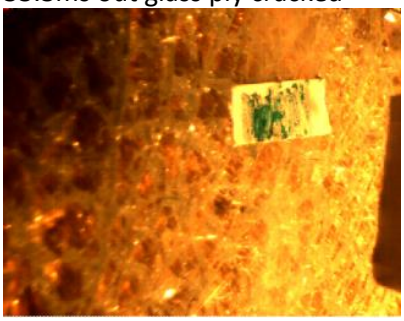

40ms inner glass ply cracked

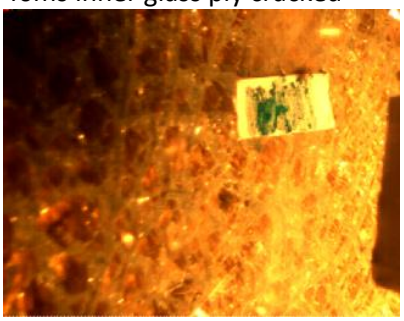

66.7ms maximum deflection

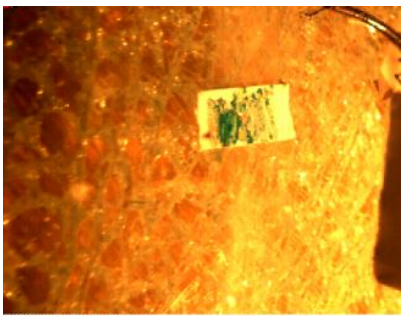

166.7ms rebounded

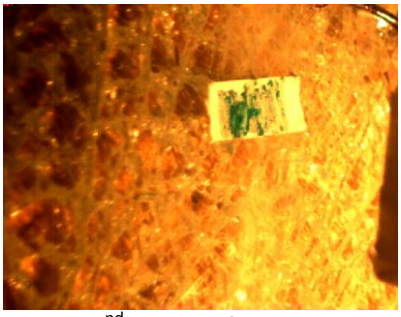

200ms 2nd peak deflection

Figure 4 High-speed camera snapshots of 12.38mm laminated pane

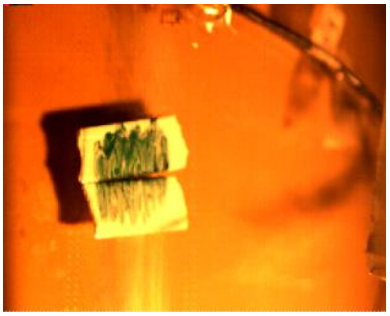

0ms impacter striked on airbag

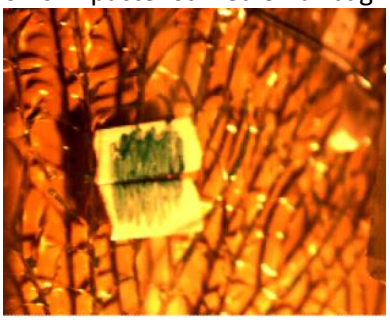

33.3ms outer glass ply cracked

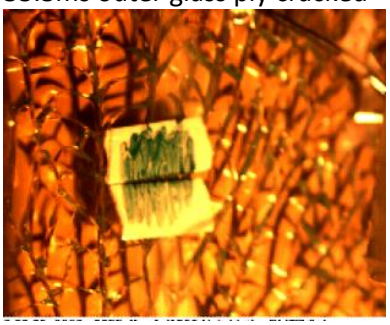

40.7ms inner glass ply cracked

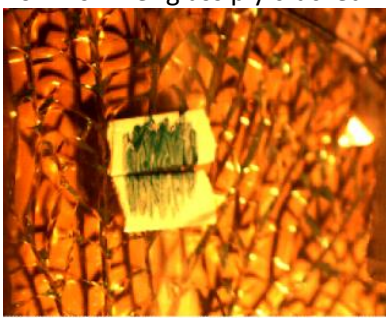

86.7ms maximum deflection

150ms rebounded

Figure 5 High-speed camera snapshots of 12.76mm laminated pane

a) 6.38mm

b) 6.76mm

c) 12.38mm

d) 12.76mm

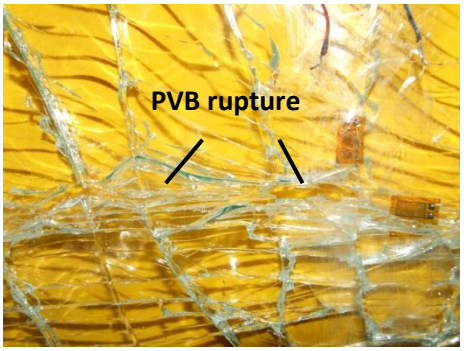

e) PVB rupture on 6.38mm pane

Figure 6 Failure patterns and details

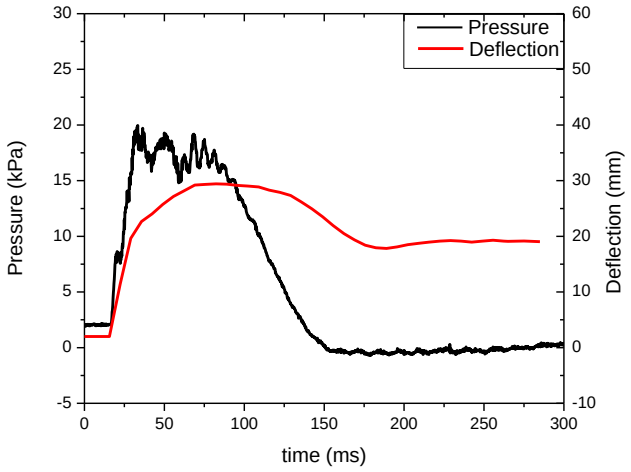

a) 6.38mm

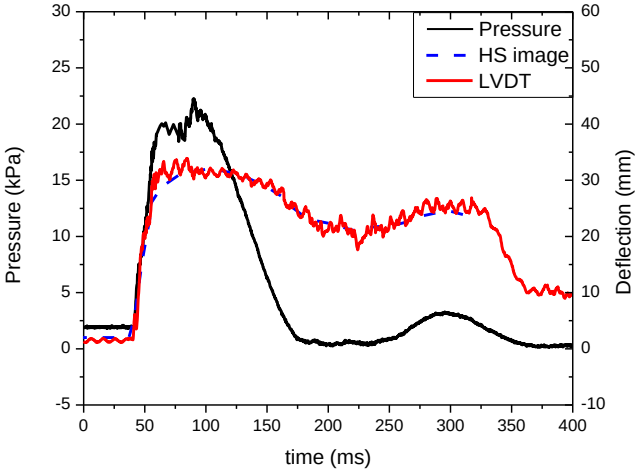

b) 6.76mm

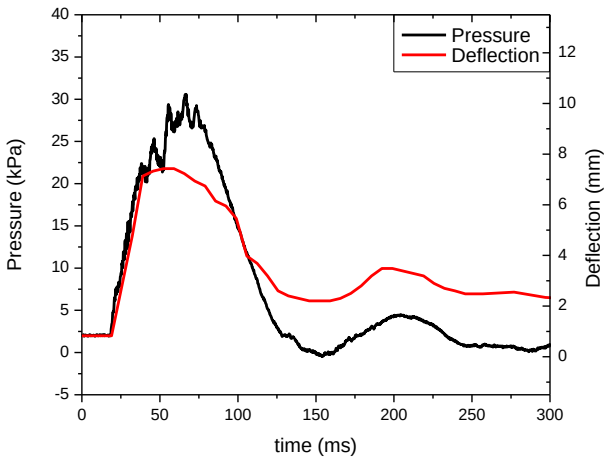

c) 12.38mm

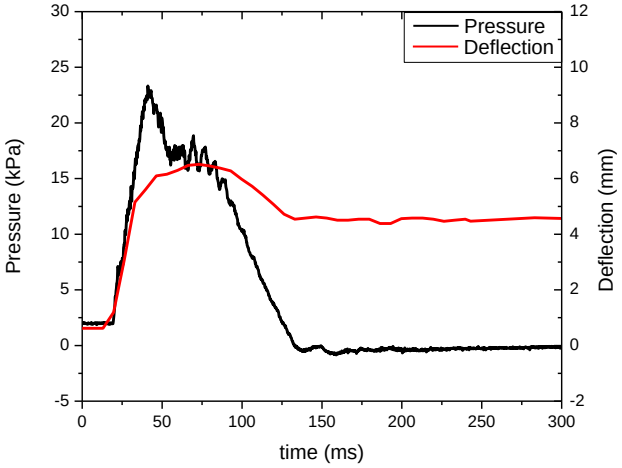

d) 12.76mm

Figure 7 Pressure and deflection time histories

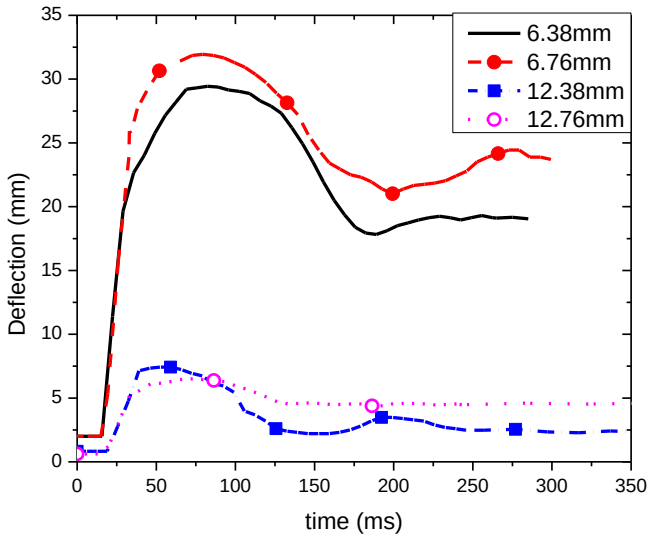

Figure 8 Responses of panes with different glass and PVB thicknesses

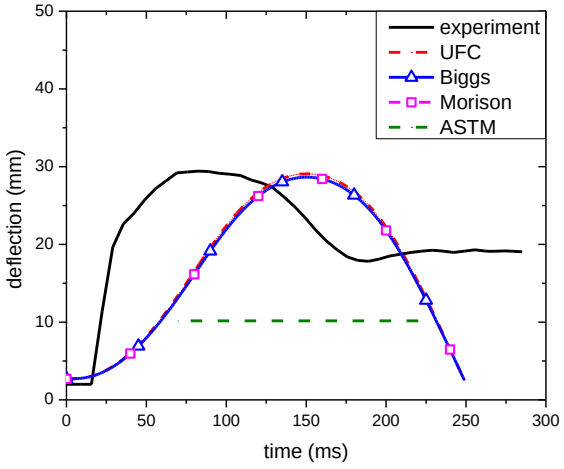

a) 6.38mm

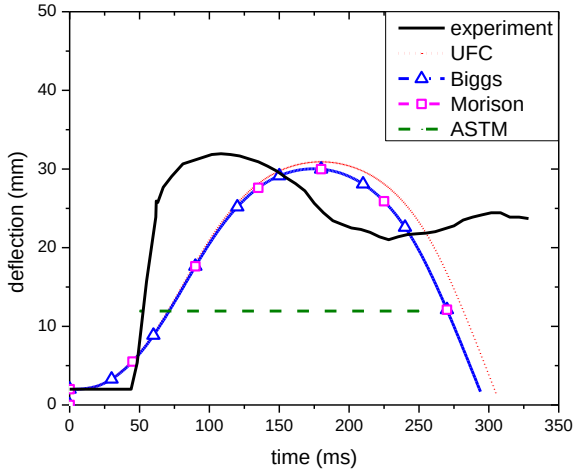

b) 6.76mm

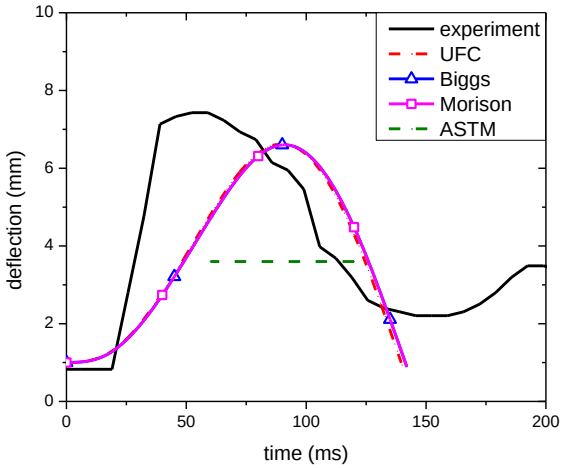

c) 12.38mm

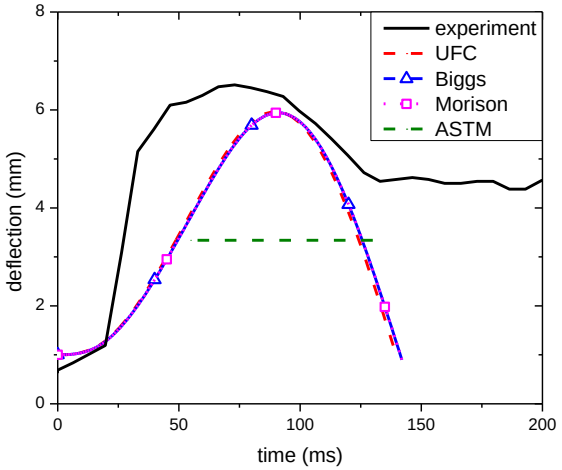

d) 12.76mm

Figure 9 Comparisons of glass responses

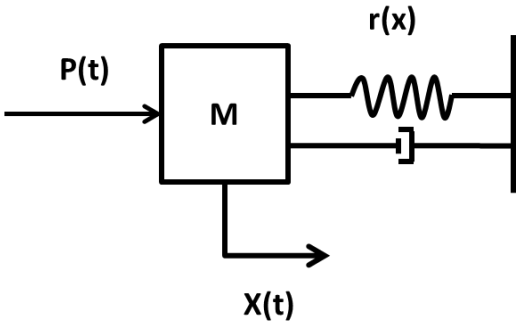

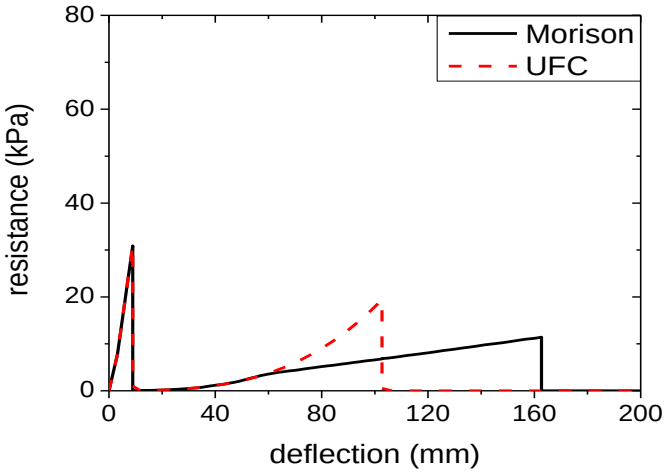

e) SDOF model

f) resistance function of 6.76mm laminated pane

Figure 10 SDOF model and 6.76mm laminated glass pane resistance function

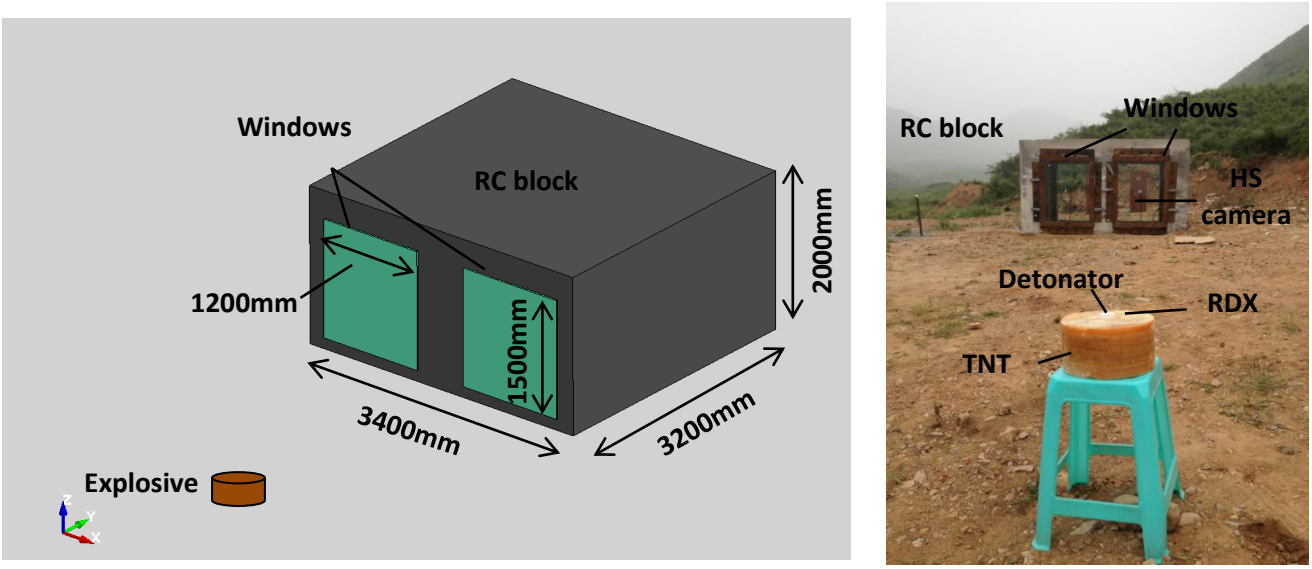

a) Schematic testing site layout

b) Image of testing site

Figure 11 Sketch of testing setup

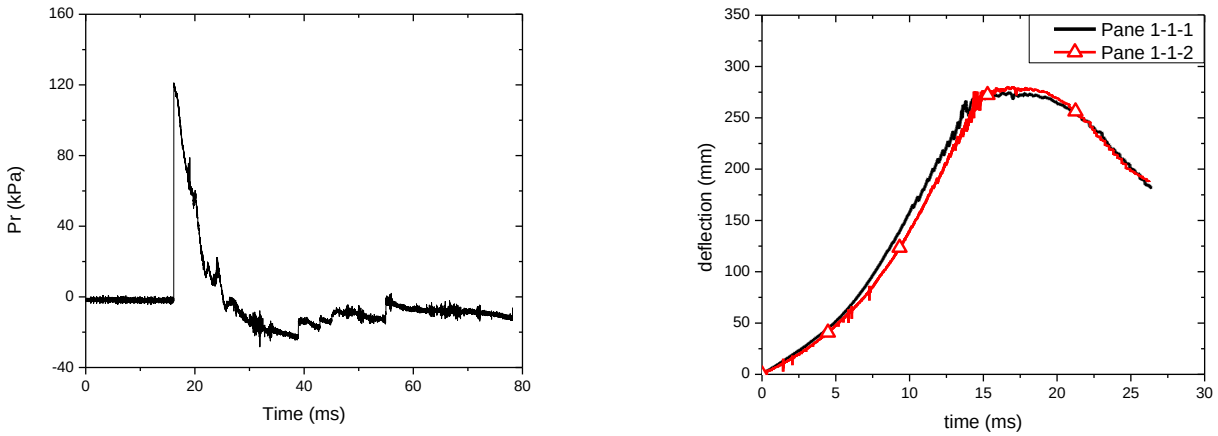

a) Test 1

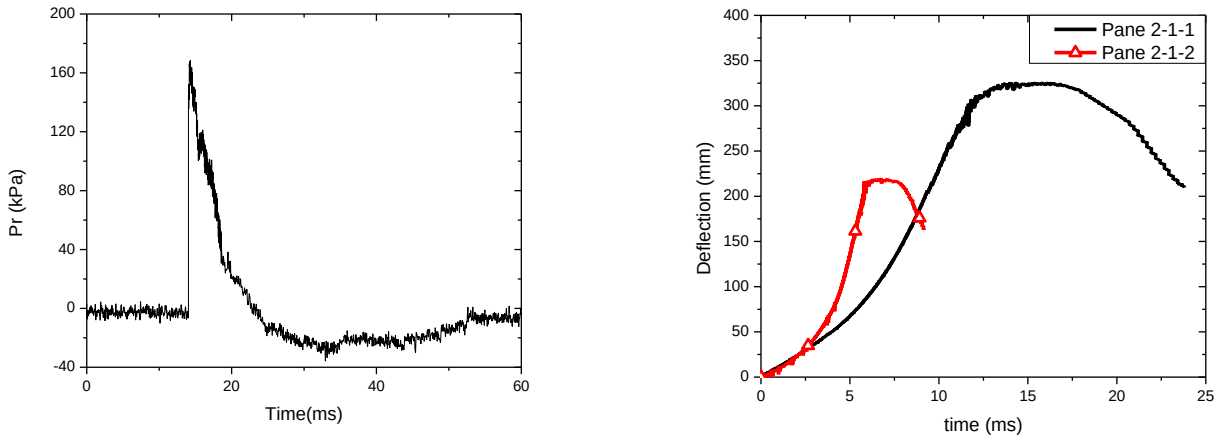

b) Test 2

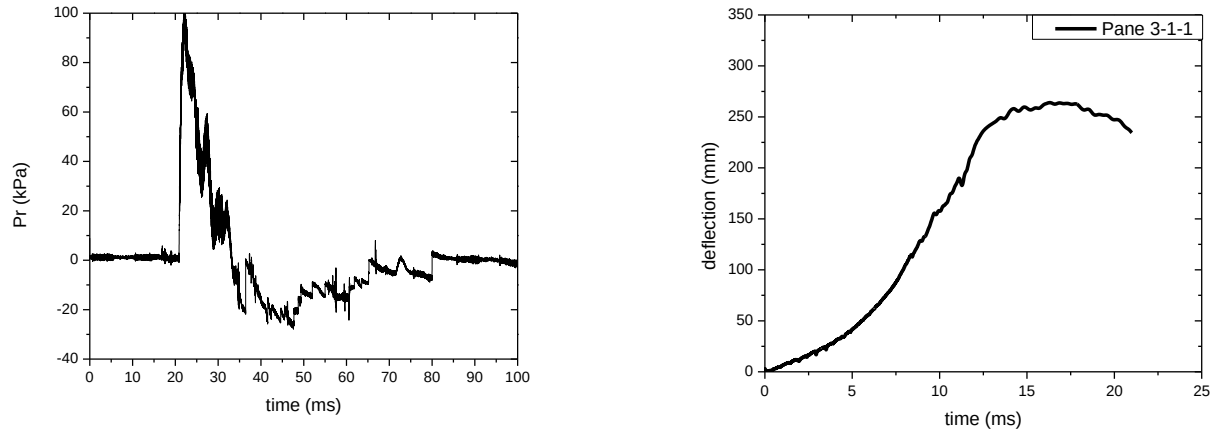

c) Test 3

Figure 12 Recorded reflected pressures and pane deflection histories

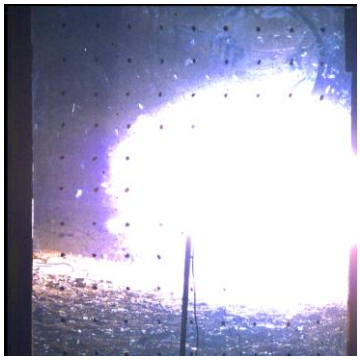

0ms charge detonated

15ms blast wave arrived

17ms back glass ply cracked

22ms glass severely damaged

30ms pane pulled out along two vertical sides

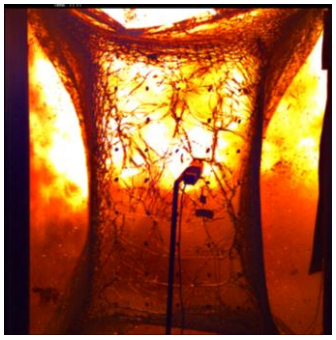

50ms pane totally pulled out of frame

a) Pane 2-1-1

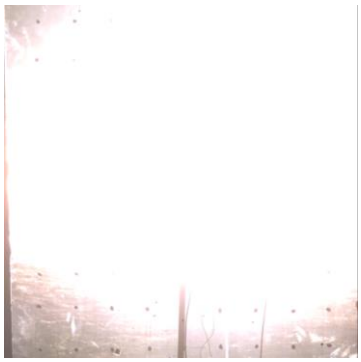

0ms charge detonated

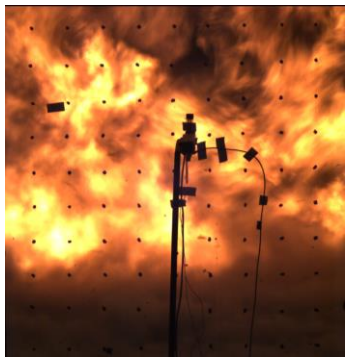

15ms blast wave arrived

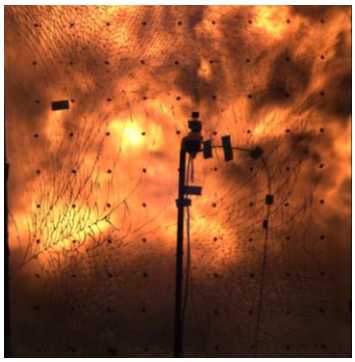

16ms back glass ply cracked

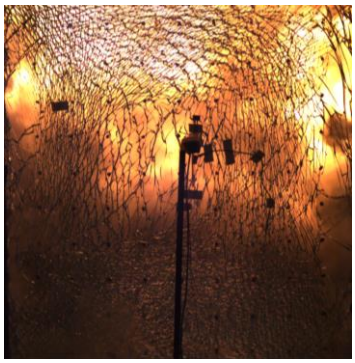

21ms glass severely damaged

31ms pane rebounded

60ms pane free vibrated

b) Pane 2-1-2

Figure 13 Snapshots of high-speed images on pane failure processes

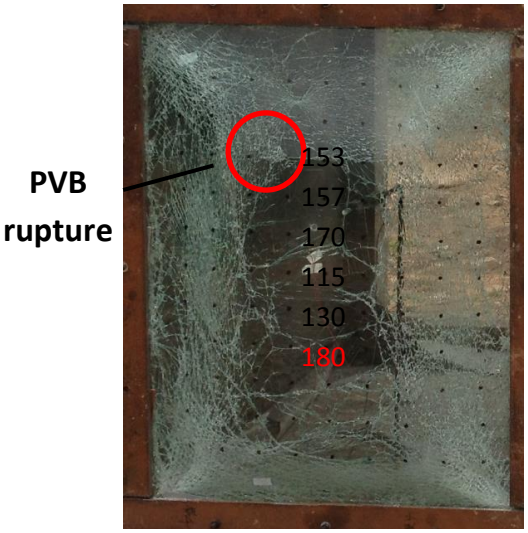

a) Pane 1-1-1 (7.52mm)

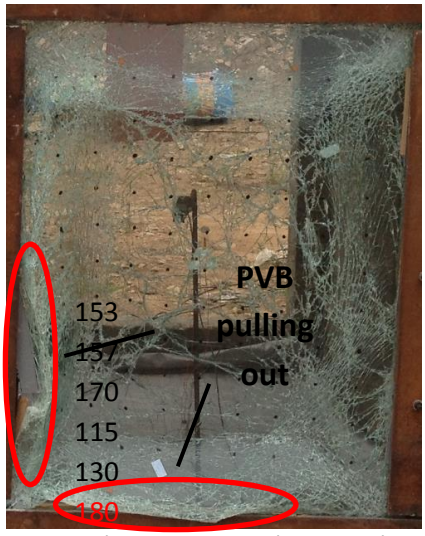

b) Pane 1-1-2 (8.28mm)

c) Pane 2-1-1 (7.52mm)

d) Pane 2-1-2 (13.52mm)

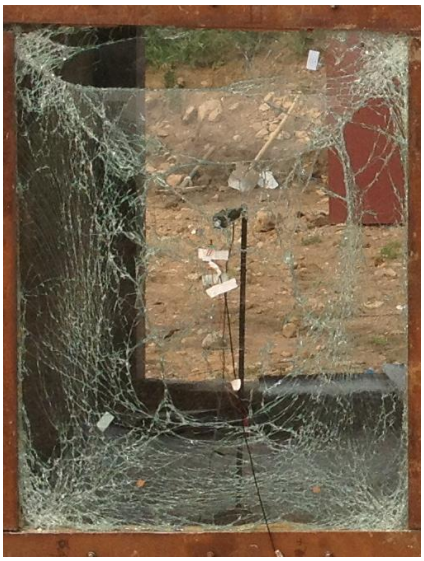

e) Pane 3-1-1 (7.52mm)

Figure 14 Pane failure patterns

Figure 15 PVB rupture observed on pane 1-1-1

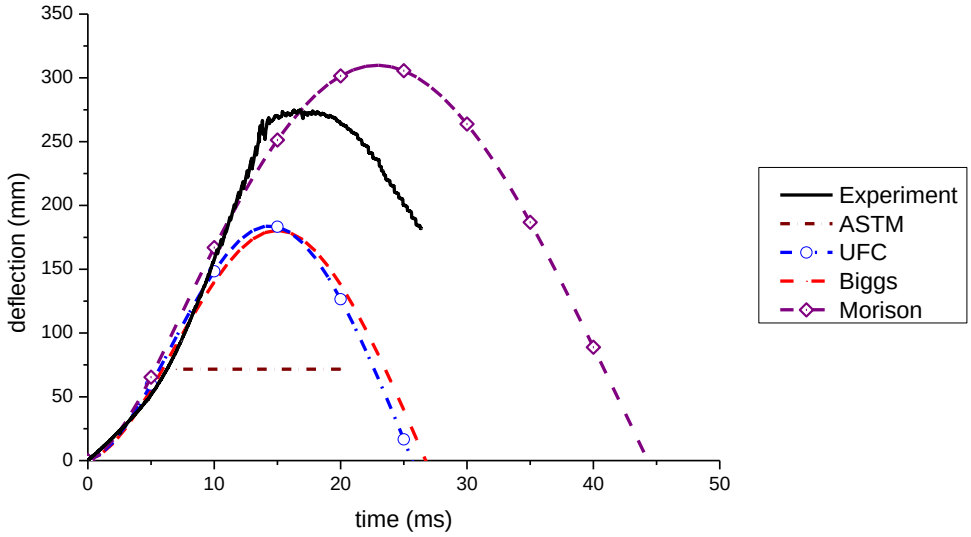

a) Pane 1-1-1

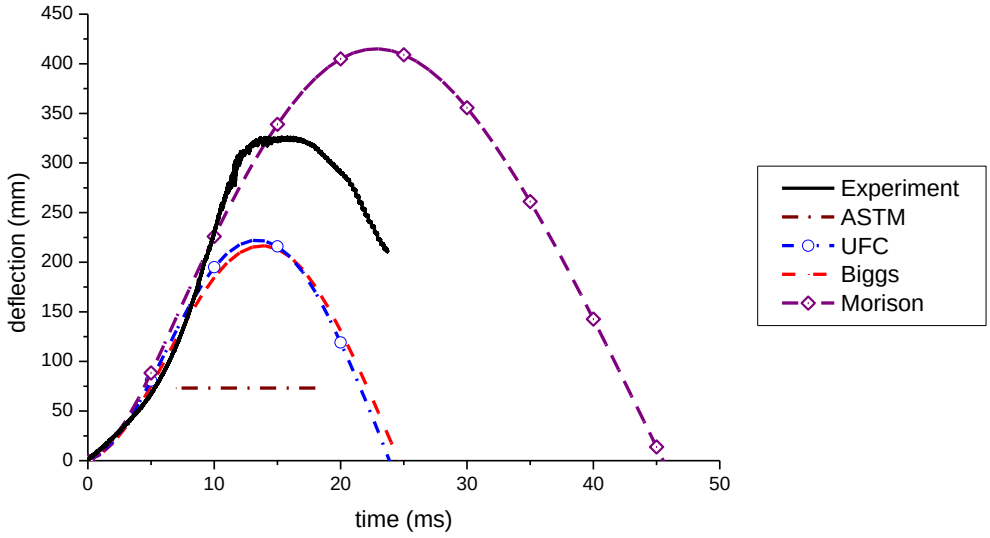

b) Pane 2-1-1

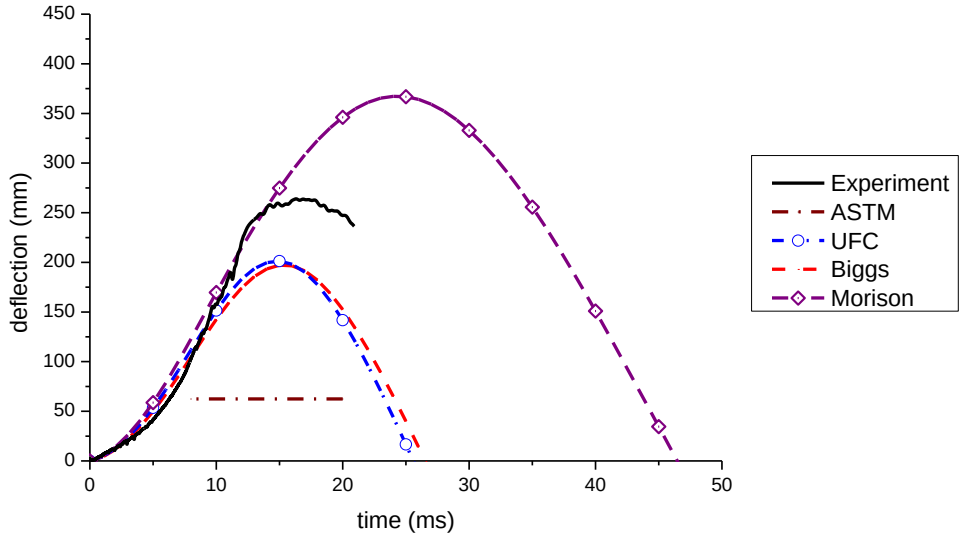

c) Pane 3-1-1

Figure 16 Comparisons of panel responses recorded in the current tests and predicted by various methods

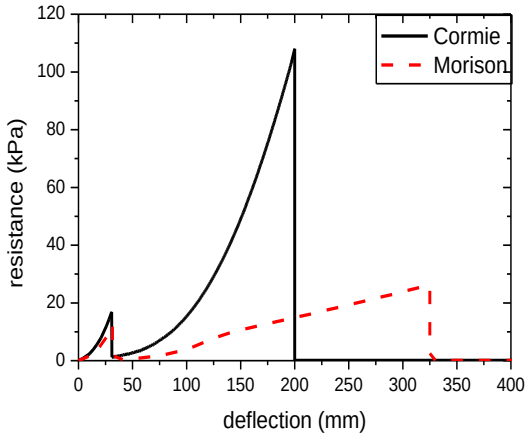

Figure 17 7.52mm laminated glass pane resistance function

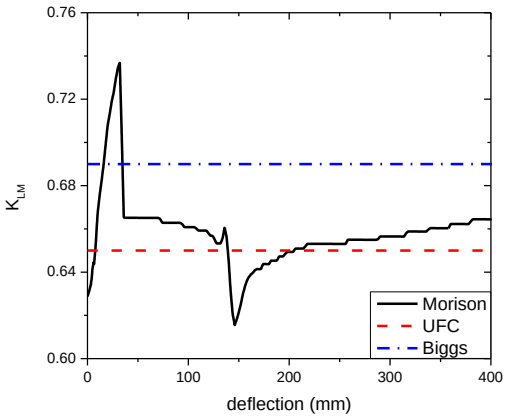

Figure 18 The load-mass factors K_{LM} in different SDOF models (with span ratio 1.25)

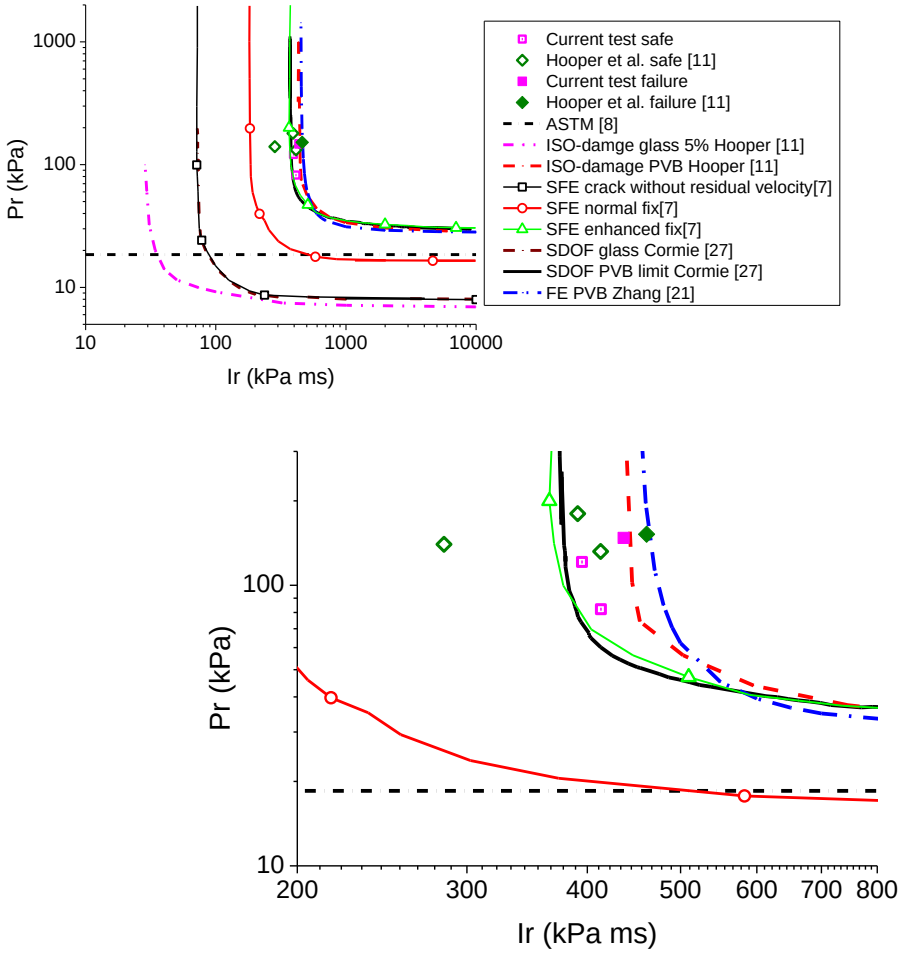

Figure 19 P-I diagrams with the current and previous testing data

Pane No.	Glass (mm)	PVB (mm)	Total thickness (mm)	Dimension (mm × mm)	Pr (kPa)	Ir (kPa-ms)	w_{max} (mm)
1	3	0.38	6.38	600 × 600	20.6	1684.0	29.4
2	3	0.76	6.76	600 × 600	21.9	1825.9	31.9
3	6	0.38	12.38	600 × 600	30.6	1984.6	7.4
4	6	0.76	12.76	600 × 600	23.7	1466.0	6.5

Table 1 Summary of laboratory impact test results

Test No.	Pane thickness (mm)	Maximum deflection (mm)				
		Experiment	ASTM	UFC	Biggs	Morison
1	6.38	29.44	10.16	29.09	28.65	28.63
2	6.76	31.95	11.94	30.92	30.05	30.03
3	12.38	7.43	3.60	6.63	6.58	6.52
4	12.76	6.51	3.34	5.97	5.95	5.88

Table 2 Summary of pane maximum deflections in laboratory tests

Test No.	Pane No.	Glass thickness (mm)	PVB thickness (mm)	Size (mm × mm)	Boundary condition	W (kg)	R (m)
1	1-1-1	3	1.52	1500 × 1200	Fixed	10	10
1	1-1-2	3	2.28	1500 × 1200	Fixed	10	10
2	2-1-1	3	1.52	1500 × 1200	Fixed	10	9
2	2-1-2	6	1.52	1500 × 1200	Fixed	10	9
3	3-1-1	3	1.52	1500 × 1200	Fixed	10	12.3

Note: W stands for the weight of TNT explosive, and R stands for the explosive stand-off distance.

Table 3 Summary of window specimens in field blasting tests

Test No.	W (kg)	R (m)	Positive phase					
			Pr (kPa)			Ir (kPa-ms)		
			Field Test	UFC	Var.	Field Test	UFC	Var.
1	10	10	121.1	117.2	3%	395.0	293.9	34%
2	10	9	168.6	147.1	15%	476.1	330.7	44%
3	10	12.3	82.2	78.1	5%	413.3	339.3	22%

Test No.	W (kg)	R (m)	Negative phase					
			Pr (kPa)			Ir (kPa-ms)		
			Field Test	UFC	Var.	Field Test	UFC	Var.
1	10	10	-28.4	-16.3	74%	319.7	92.5	246%
2	10	9	-35.8	-18.3	96%	543.5	101.4	436%
3	10	12.3	-17.5	-13.1	34%	261.7	212.8	23%

Table 4 Summary of recorded blast loads and UFC estimations

Test No.	Pane No.	Glass thickness (mm)	PVB thickness (mm)	Pr (kPa)	Ir (kPa-ms)	w_{max} (mm)
1	1-1-1	3	1.52	121	395	275
1	1-1-2	3	2.28	121	395	280
2	2-1-1	3	1.52	169	476	326
2	2-1-2	6	1.52	169	476	220
3	3-1-1	3	1.52	82	413	264

Table 5 Summary of window responses in field blasting tests

Pane No.	w_{max} (mm)				
	Experiment	ASTM	UFC3	Biggs	Morison
1-1-1	275	72	181	184	310
2-1-1	326	73	222	229	415
3-1-1	264	62	201	204	367

Table 6 Summary of maximum deflections